were exposed to serial 10-fold dilutions of type 14 rhinovirus at a dose ranging from 10^1 to 10^5 $TCID_{50}$ units/ml, containing procaterol or vehicle for 1 h at 33 °C. After exposure to type 14 rhinovirus, cells were rinsed with PBS, and a fresh medium without the addition of procaterol was replaced. Cells in the tubes were then cultured at 33 °C by rolling in an incubator.

We collected the supernatant fluids at 1, 12, and 24 h after type 14 rhinovirus infection with the methods described above (Collection of supernatant fluids for measurements). Supernatant fluids were also collected at 3 days (72 h), 5 days (120 h) and 7 days (168 h) after type 14 rhinovirus infection.

Because we found in the preliminary experiments that the supernatant fluids collected at 3 days (72 h) after infection showed maximum viral titers, we measured the rhinovirus titers in the supernatant fluids collected at 3 days (72 h) after infection with the human embryonic fibroblast cell assay described above in order to assess whether infection occurred at each dose (10^1, 10^2, 10^3, 10^4 or 10^5 $TCID_{50}$ units/ml) of type 14 rhinovirus used. After addition of virus-containing supernatant fluids to the fibroblast cells, the presence of the typical cytopathic effects of rhinovirus was observed for 7 days (168 h) (Yamaya et al., 2007).

2.10. Measurement of ICAM-1 expression

The mRNA of ICAM-1 was examined with the two-step real-time RT-PCR analysis with the methods described above (Quantification of rhinovirus RNA), by using a forward primer (5′-GCACTTCTGTTTCCCAG-GAGC-3′) and a reverse primer (5′-CGGACACCCAAAGTAG TCGGT-3′). Taqman probe (5′-[FAM] CCTTTAACCGTTATCCGCCA [TAMRA]-3′] was designed for ICAM-1. The expression of ICAM-1 mRNA was also normalized to the constitutive expression of rRNA. Concentrations of sICAM-1 in supernatant fluids were measured with the enzyme immunoassay (EIA) (Yamaya et al., 2007).

2.11. Measurement of changes in acidic endosomes

The distribution and the fluorescence intensity of acidic endosomes in the cells were measured as previously described with a dye, LysoSensor DND-189 (Molecular Probes, Eugene, OR, USA) (Suzuki et al., 2001). Live-cell imaging was performed. The cells on coverslips in Petri dishes were observed with a fluorescence microscope (OLYMPUS IX70; OLYMPUS Co. Ltd., Tokyo, Japan). The excitation wavelength was 443 nm, and the emitted light from the cells was detected through a 505-nm filter. The fluorescence intensity was calculated using a fluorescence image analyzer system (Lumina Vision®; Mitani Co. Ltd., Fukui, Japan) equipped with a fluorescence microscope. Fluorescence intensity of acidic endosomes was measured in 100 human tracheal epithelial cells, and the mean value of fluorescence intensity was expressed as a percentage of the control value compared with the fluorescence intensity of the cells before any treatment.

We studied the effects of a long period of treatment with procaterol (0.1 μM, 72 h) on acidic endosomes, because cells were pretreated with procaterol for 3 days (72 h) before type 14 rhinovirus infection. Furthermore, to examine the time-dependent effects of procaterol on acidic endosomes, cells were treated with procaterol (0.1 μM) for the time ranging from 0 h to 3 days (72 h).

To examine the concentration-dependent effects of procaterol on acidic endosomes, cells were treated with procaterol at concentrations ranging from 1 nM to 100 nM.

2.12. Measurement of cytokine production

We measured interleukin-1β, interleukin-6, and interleukin-8 of supernatant fluids by specific enzyme-linked immunosorbent assays (ELISAs) (Yamaya et al., 2007) in duplicate human tracheal epithelial cells in plastic tubes at all time points.

2.13. NF-kappa B assay

Nuclear extracts from human tracheal epithelial cells were prepared using a TransFactor extraction kit (BD Bioscience/CLONTECH, Mountain View, CA, USA) according to manufacturer's instructions. After centrifugation at 20,000×g for 5 min at 4 °C, nuclear extracts were assayed for p50, p65, and c-Rel content. An equal amount of nuclear lysate was added to incubation wells precoated with the DNA-binding consensus sequence. The presence of translocated p50, p65, and c-Rel subunit was assayed by using a TransFactor Family Colorimetric Kit-NFκB (BD Bioscience/CLONTECH) according to the manufacturer's instructions (Fiorucci et al., 2002). Plates were read at 655 nm and results are expressed as OD, which shows quantitative levels of NF-kB subunits (Fiorucci et al., 2002).

2.14. Western blot analysis

Western blot analysis for the degradation of inhibitory kappa B-α (IκB-α) and the analysis of the amount of phosphorylated IκB-α (p-IκB-α) and β-actin were performed with the methods described previously (Kim et al., 2008) with some modification. Total cellular proteins from human tracheal epithelial cells before and after type 14 rhinovirus infection in the presence or absence of procaterol (0.1 μM) and a selective β_2-adrenergic receptor antagonist ICI 118551 (1 μM) were harvested and lysed in modified radioimmunoprecipitation assay (RIPA) buffer (1% NP-40, 0.25% sodium deoxycholate, 150 mM NaC1, 20 mM Tris, pH 7.5, and 10 mM EDTA) supplemented with phosphatase and protease inhibitors.

Protein concentrations were determined using the Bio-Rad protein assay reagent, according to the manufacturer's instructions. Twenty micrograms of cellular proteins from treated or untreated cell extracts were separated on 10% SDS-polyacrylamide gels and electroblotted onto nitrocellulose membranes that were incubated for 2 h with blocking solution (5% skim milk) at 4 °C and then with primary antibody overnight. Primary antibodies used in this study were a monoclonal rabbit anti-phospho-IκB-α (Ser32) antibody (1:1000 dilution; Cell Signaling Technology, Danvers, MA, USA), a polyclonal rabbit anti-IκB-α (C-21) antibody (1:200 dilution; Santa Cruz Biotechnonogy, Santa Cruz, CA, USA), and a monoclonal mouse anti-β-actin antibody (1:10,000 dilution; Sigma-Aldrich, St. Louis, MO, USA). Blots were then washed four times with Tween 20/Tris-buffered saline (TTBS), incubated with one of the following secondary antibodies for 1 h at room temperature: peroxidase-conjugated anti-rabbit IgG (1:1000 dilution; DakoCytomation, Glostrup, Denmark) for p-IκB-α and IκB-α or peroxidase-conjugated anti-mouse IgG (1:10,000 dilution; Jackson Immuno Research Laboratories, Avondale, PA, USA) for β-actin. Blots were rewashed three times with TTBS, and chemiluminescence was detected using an Amersham ECL Plus western blotting detection kit (GE Healthcare, Waukesha, WI, USA) and a LAS-1000 lumino image analyzer (Fujifilm, Tokyo, Japan). The results were quantified using ImageJ 1.42 software (http://rsb.info.nih.gov/ij/). The data were obtained by dividing the results in each culture condition by the results of β-actin.

2.15. Cyclic AMP assay

Intracellular cyclic AMP (cAMP) levels were measured as previously reported (Chiulli et al., 2000) with the cAMP-Screen™ System (Applied Biosystems). Human tracheal epithelial cells, cultured in a 96-well plate, were treated with either procaterol (0.1 μM), ICI 118551 (1 μM), procaterol (0.1 μM) plus ICI 118551 (1 μM), or vehicle (0.01% ethanol) for either 5 min, 10 min, 20 min, or 3 days (72 h). Intracellular cAMP was then extracted by adding Assay/Lysis buffer to the cells in the wells, and the extracted samples were incubated at 37 °C for 30 min. The samples containing cAMP were incubated with anti-cAMP antibody in the wells of the 96-well plates at room

temperature for 60 min. The combined cAMP with anti-cAMP antibody, which was adhered to the bottom of the wells, was then rinsed with wash buffer, and 100 μl/well of CSPD®/Sapphire-II™ RTU substrate/enhancer solution was added to the wells and incubated for 30 min. The signal was measured in a luminometer (Luminoscan acent; ThermoFisher Scientific Co., MA, USA) for 1 s/well. The standard curve was obtained by using 10-fold dilutions of cAMP at the concentrations ranging from 0.6×10^{-3} pmol to 6×10^{3} pmol in each well of 96-well plates. Results are shown as pmol/well according to the standard curve and expressed as pmol/mg protein after being normalized to the amount of protein in the cells in the wells.

2.16. Statistical analysis

Results are expressed as means ± S.E.M. Statistical analysis was performed using a one-way analysis of variance (ANOVA). Subsequent post-hoc analysis was made using Bonferroni's method. For all analyses, values of $P<0.05$ were assumed to be significant. n refers to the number of donors (tracheae) from which cultured epithelial cells were used.

3. Results

3.1. Effects of procaterol on rhinovirus infection in human tracheal epithelial cells

Exposing confluent human tracheal epithelial cell monolayers to type 14 rhinovirus (5.0×10^{-2} $TCID_{50}$ units/cell) consistently led to infection. No detectable virus was revealed at 1 h after infection, but type 14 rhinovirus was detected in culture medium at 12 h, and the viral content progressively increased between 1 and 12 h after infection (Fig. 1). Evidence of continuous viral production was obtained by demonstrating that each of the supernatant fluids collected during either 12 h to 24 h (1 day), 1 day (24 h) to 3 days (72 h), 3 days (72 h) to 5 days (120 h), or 5 days (120 h) to 7 days (168 h) after infection contained significant levels of type 14 rhinovirus (Fig. 1). The viral titer levels in supernatant fluids increased significantly with time for the first 3 days (72 h) ($P<0.05$ by ANOVA). Furthermore, in the tracheal cells from subjects whose cells were infected with rhinovirus, the supernatant fluids collected during 1 (24 h) to 3 days (72 h) after infection contained consistent levels of type 14 rhinovirus (4.53 ± 0.18 log $TCID_{50}$ units/ml/24 h, n = 38).

Treatment of the cells with procaterol (0.1 μM) significantly decreased the viral titers of type 14 rhinovirus in supernatant fluids from 12 h after infection (Fig. 1). Furthermore, a selective β_2-adrenergic receptor antagonist ICI 118551 (1 μM) reversed the inhibitory effects of procaterol on type 14 rhinovirus titer levels (Fig. 1), whereas ICI 11851 alone did not change the titer levels (data not shown).

Type 14 rhinovirus titer levels in supernatant fluids of the cells, collected from 13 ex-smokers over 1 day (24 h) to 3 days (72 h) after infection, did not differ from those of 25 patients who had never smoked (4.58 ± 0.32 log $TCID_{50}$ units/ml/24 h *vs* 4.50 ± 0.21 log $TCID_{50}$ units/ml/24 h, respectively, $P>0.02$). Likewise, type 14 rhinovirus titer levels in supernatant fluids of the cells from three patients complicated with COPD did not differ from those from 35 patients without COPD (data not shown). No virus was detected in supernatant fluids after infection of ultraviolet (UV)-inactivated type 14 rhinovirus (data not shown).

Treatment with procaterol (0.1 μM) for 3 days (72 h) did not change the viability (99 ± 1% in procaterol *vs* 98 ± 1% in vehicle, n = 5, $P>0.50$), as assessed by the exclusion of trypan blue. Furthermore, until 7 days (168 h) after the start of cell culture, cells made confluent sheets in the tubes in both the culture medium alone and the medium containing procaterol at the same time point. The cell number of confluent sheets cultured in the medium supplemented with procaterol (0.1 μM) did not differ from that in the medium alone ($2.1\pm0.3\times10^{6}$ of cells/tube in procaterol *vs* $2.2\pm0.3\times10^{6}$ of cells/tube in vehicle, n = 5, $P>0.50$). When LDH concentrations in supernatant fluids 3 days (72 h) after procaterol treatment (0.1 μM) were measured, treatment with procaterol (0.1 μM) for 3 days (72 h) did not change the LDH concentration (32 ± 3 IU/l/24 h in procaterol *vs* 33 ± 3 IU/l/24 h IU/ml in vehicle, n = 5, $P>0.50$).

Procaterol inhibited type 14 rhinovirus infection concentration-dependently. The maximum effect was obtained at 0.1 μM, 1.0 μM, and 10 μM, and the minimum effect was obtained at 3 nM (Fig. 2).

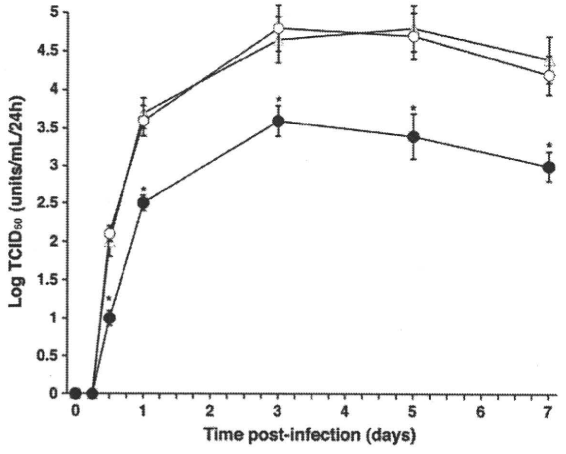

Fig. 1. The time course of viral release in supernatant fluids of human tracheal epithelial cells obtained at different times after exposure to 5.0×10^{-2} $TCID_{50}$ units/cell of type 14 rhinovirus in the presence of procaterol (0.1 μM) (closed circles), the vehicle of procaterol (ethanol, 0.01%) (open circles), or the presence of procaterol (0.1 μM) plus ICI 118551 (1 μM) (open triangles). The epithelial cells isolated from the same donors were treated with either procaterol, vehicle, or procaterol plus ICI 118551. To examine whether supernatant fluids contain significant amount of rhinovirus, cytopathic effects on human embryonic fibroblast cells were observed for 7 days (168 h) after placing the supernatant fluids on the fibroblast cells. The rates of change in type 14 rhinovirus concentration in the supernatant fluids are expressed as $TCID_{50}$ units/ml/24 h. Results are means ± S.E.M. from 6 different tracheae (2 ex-smokers and 4 non-smokers). Significant differences from viral infection alone are indicated by *$P<0.05$.

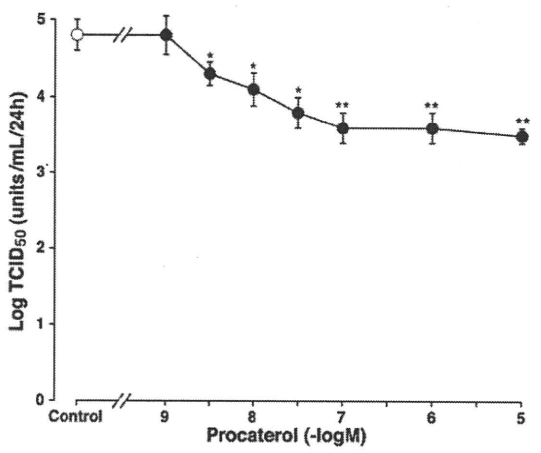

Fig. 2. Concentration-response effects of procaterol on the viral release in supernatant fluids collected over 1 day (24 h) to 3 days (72 h) after infection. The cells were treated with procaterol (closed circles) or vehicle (Control; ethanol, 0.01%, open circle) from 3 days (72 h) before type 14 rhinovirus infection until the end of the experiments after type 14 rhinovirus infection. The epithelial cells isolated from the same donors were treated with either procaterol or vehicle. In order to examine whether supernatant fluids contain significant amount of rhinovirus, cytopathic effects on human embryonic fibroblast cells were observed for 7 days (168 h) after placing the supernatant fluids on the fibroblast cells. The rates of change in type 14 rhinovirus concentration in the supernatant fluids are expressed as $TCID_{50}$ units/ml/24 h. Results are means ± S.E.M. from 10 different tracheae (4 ex-smokers and 6 non-smokers). Significant differences from vehicle alone (Control) are indicated by *$P<0.05$ and **$P<0.01$.

3.2. Effects of procaterol on viral RNA by real-time RT-PCR

Further evidence of the inhibitory effects of procaterol on type 14 rhinovirus RNA replication in human tracheal epithelial cells was provided by real-time quantitative RT-PCR analysis. The RNA extraction was performed at 1 day (24 h), 3 days (72 h) and 5 days (120 h) after type 14 rhinovirus infection. Type 14 rhinovirus RNA in the cells was consistently observed from 1 day (24 h) after infection, increased with time after infection (Fig. 3), and maximum rhinovirus RNA replication was observed at 3 days (72 h) after infection (data at 120 h not shown), whereas type 14 rhinovirus RNA in the cells was not observed before infection (data not shown). Procaterol (0.1 μM) decreased the type 14 rhinovirus RNA at 1 day (24 h) and at 3 days (72 h) after infection (Fig. 3).

On the other hand, ICI 118551 (1 μM) reversed the inhibitory effects of procaterol on the type 14 rhinovirus RNA replication, whereas ICI 118551 alone did not change it (Fig. 3). The amount of type 14 rhinovirus RNA in the cells treated with ICI 118551 (1 μM) alone did not differ from that in the cells treated with vehicle (ethanol, 0.01%) at 1 day (24 h) and at 3 days (72 h) after type 14 rhinovirus infection (Fig. 3). In contrast, the amount of type 14 rhinovirus RNA in the cells treated with procaterol (0.1 μM) plus ICI 118551 (1 μM) were significantly higher than that in the cells treated with procaterol alone and did not differ from that in the cells treated with vehicle at 1 day (24 h) and at 3 days (72 h) after type 14 rhinovirus infection (Fig. 3).

3.3. Effects of procaterol on susceptibility to rhinovirus infection

Treatment of the cells with procaterol (0.1 μM) decreased the susceptibility of the cells to infection by type 14 rhinovirus. When viral release was measured using supernatant fluids collected 3 days (72 h) after rhinovirus infection, the minimum dose of type 14 rhinovirus necessary to cause infection in the cells treated with procaterol (0.1 μM, 72 h) (3.2 ± 0.2 log $TCID_{50}$ units/ml, $n = 5$, $P<0.05$) was significantly higher than that in the cells treated with the vehicle of procaterol (ethanol, 0.01%) (2.2 ± 0.2 log $TCID_{50}$ units/ml, $n = 5$) (Fig. 4A). Likewise, when viral release was measured using supernatant fluids collected 5 days (120 h) and 7 days (168 h) after type 14 rhinovirus infection, the minimum dose of rhinovirus necessary to cause infection in the cells treated with procaterol and that in the cells treated with the vehicle of procaterol were the same values as those in supernatant fluids collected at 3 days (72 h) after rhinovirus infection (data not shown).

A selective β_2-adrenergic receptor antagonist ICI 118551 (1 μM) itself did not change the minimum dose of type 14 rhinovirus necessary to cause infection in the cells, and did not affect the susceptibility (data not shown). In contrast, ICI 118551 reversed the effects of procaterol on susceptibility to type 14 rhinovirus infection. Treatment of the cells with ICI 118551 (1 μM, 72 h) plus procaterol

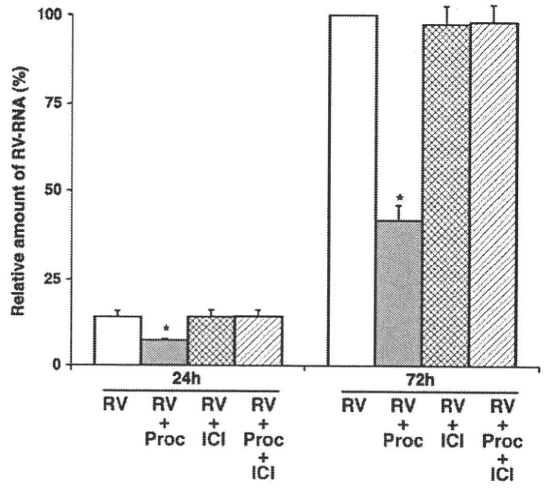

Fig. 3. Replication of viral RNA in human tracheal epithelial cells at 1 day (24 h) or 3 days (72 h) after infection with type 14 rhinovirus in the presence of procaterol (0.1 μM) (RV + Proc), vehicle (0.01% ethanol) (RV), ICI 118551 (1 μM) (RV + ICI), or the presence of procaterol (0.1 μM) plus ICI 118551 (1 μM) (RV + Proc + ICI) as detected by real-time quantitative RT-PCR. The epithelial cells isolated from the same donors were treated with either procaterol, vehicle, ICI 118551, or procaterol plus ICI 118551. Results are expressed as the relative amount of RNA expression (%) compared with that of maximal rhinovirus RNA at day 3 (72 h) in the cells treated with vehicle, and reported as means ± S.E.M. from five samples (2 ex-smokers and 3 non-smokers). Significant differences from treatment with a vehicle (RV) at each time are indicated by $^*P<0.05$.

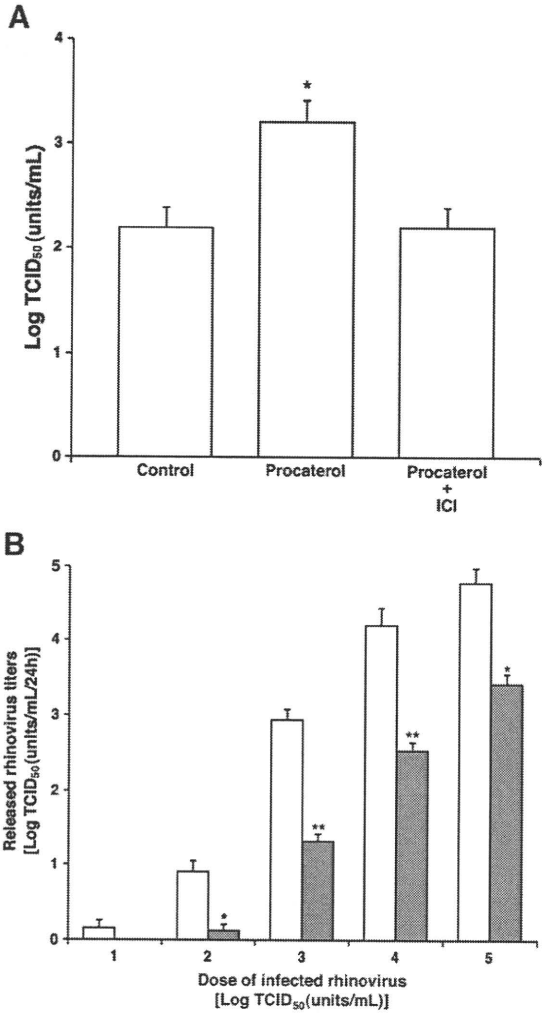

Fig. 4. (A) The minimum dose of type 14 rhinovirus necessary to cause infection in the human tracheal epithelial cells treated with either procaterol (0.1 μM, 72 h), vehicle (Control, 0.01% ethanol), or procaterol (0.1 μM) plus ICI 118551 (1 μM) (Procaterol + ICI). The epithelial cells isolated from the same donors were treated with either procaterol, vehicle, or procaterol plus ICI 118551. In order to examine whether supernatant fluids contain significant amount of rhinovirus, cytopathic effects on human embryonic fibroblast cells were observed for 7 days (168 h) after placing the supernatant fluids on the fibroblast cells. The minimum dose of type 14 rhinovirus necessary to cause infection is expressed as $TCID_{50}$ units/ml. Results are means ± S.E.M. from seven different tracheae (2 ex-smokers and 5 non-smokers). Significant differences from vehicle alone (Control) are indicated by $^*P<0.05$. (B) Viral release in supernatant fluids collected during 24 h (1 day) to 72 h (3 days) after infection with type 14 rhinovirus at a dose ranging from 10^1 to 10^5 $TCID_{50}$ units/ml in the presence of procaterol (0.1 μM) (gray columns) or the vehicle of procaterol (ethanol, 0.01%) (open columns). The rates of change in type 14 rhinovirus concentration in the supernatant fluids are expressed as $TCID_{50}$ units/ml/24 h. Results are means ± S.E.M. from seven different tracheae (2 ex-smokers and 5 non-smokers). Significant differences from viral infection alone at each dose of type 14 rhinovirus are indicated by $^*P<0.05$ and $^{**}P<0.01$.

(0.1 μM, 72 h) decreased the minimum dose of type 14 rhinovirus necessary to cause infection in the cells (2.2 ± 0.2 log $TCID_{50}$ units/ml, $n = 5$) as compared with the dose in the cells treated with procaterol ($P<0.05$) (Fig. 4A), to the levels in the cells treated with the vehicle of procaterol (ethanol, 0.01%) (Fig. 4A).

Type 14 rhinovirus titer levels in supernatant fluids collected at 3 days (72 h) after rhinovirus infection increased with the dose of rhinovirus infected to epithelial cells ($P<0.05$ by ANOVA) (Fig. 4B) Furthermore, treatment with procaterol (0.1 μM, 72 h) reduced the type 14 rhinovirus titers in supernatant fluids at each dose of rhinovirus infection (Fig. 4B).

3.4. Effects of procaterol on the expression of ICAM-1

Procaterol (0.1 μM, 72 h) reduced the baseline ICAM-1 mRNA expression in the cells by about 40% compared with that of the cells treated with the vehicle of procaterol (ethanol, 0.01%) before type 14 rhinovirus infection (Fig. 5A). Furthermore, concentrations of sICAM-1 in supernatant fluids in the cells treated with procaterol (0.1 μM) were significantly lower than those in the cells treated with the vehicle of procaterol before type 14 rhinovirus infection (Fig. 5B).

ICI 118551 (1 μM) itself did not change ICAM-1 mRNA expression and sICAM-1 release in supernatant fluids (Fig. 5A and B). In contrast, ICI 118551 (1 μM) reversed the inhibitory effects of procaterol on the ICAM-1 mRNA expression in the cells and sICAM-1 release in supernatant fluids (Fig. 5A and B). The ICAM-1 mRNA expression and concentrations of sICAM-1 in supernatant fluids in the cells treated with procaterol (0.1 μM) plus ICI 118551 (1 μM) were significantly higher than those in the cells treated with procaterol (0.1 μM) alone and did not differ from those in the cells treated with the vehicle (ethanol, 0.01%) before type 14 rhinovirus infection (Fig. 5A and B).

3.5. Effects of procaterol on the acidification of endosomes

Acidic endosomes in human tracheal epithelial cells were stained green with LysoSensor DND-189 (Fig. 6A–C) as shown previously (Yamaya et al., 2007). Treatment with the vehicle (ethanol, 0.01%) for 3 days (72 h) did not change the number of acidic endosomes with green fluorescence in the cells (Fig. 6A and B) and the fluorescence intensity from acidic endosomes compared with that in the cells before any treatment (Fig. 6D). In contrast, treatment with procaterol (0.1 μM, 72 h) reduced the number of acidic endosomes with green fluorescence in the cells (Fig. 6C) and the fluorescence intensity from acidic endosomes in the cells compared with cells treated with vehicle of procaterol (ethanol, 0.01%) and before any treatment (Fig. 6D).

Furthermore, treatment of the cells with ICI 118551 (1 μM, 72 h) reversed the inhibitory effects of procaterol on the number of acidic endosomes with green fluorescence in the cells (data not shown) and the fluorescence intensity from acidic endosomes, while ICI 118551 alone did not change the fluorescence intensity (Fig. 6D).

The inhibitory effects of procaterol on the fluorescence intensity from acidic endosomes were time- and dose-dependent, and significant inhibitory effects were observed when cells were treated with procaterol (0.1 μM) for the time of 12 h or more (Fig. 6E). The maximum inhibitory effect was obtained when cells were treated with procaterol for 3 days (72 h) (Fig. 6E). The inhibitory effects of procaterol on the fluorescence intensity from acidic endosomes were also dose-dependent. Significant inhibitory effects were observed at 3 nM, and the maximum inhibitory effect was obtained at 100 nM (0.1 μM) (Fig. 6F).

3.6. Effects of procaterol on cytokine production

Procaterol (0.1 μM) reduced the baseline secretion of interleukin-1β, interleukin-6, and interleukin-8 for 24 h before type 14 rhinovirus infection compared with that in cells treated with the vehicle of procaterol (ethanol, 0.01%) (Fig. 7). Type 14 rhinovirus infection increased the secretion of interleukin-1β, interleukin-6, and interleukin-8. Maximum secretion was observed at 1 day (24 h) after type 14 rhinovirus infection in interleukin-6 and interleukin-8, and at 3 days (72 h) after the infection in interleukin-1β. Procaterol (0.1 μM) also reduced the type 14 rhinovirus infection-induced secretion of interleukin-1β, interleukin-6, and interleukin-8 compared with that in the cells treated with vehicle of procaterol (Fig. 7).

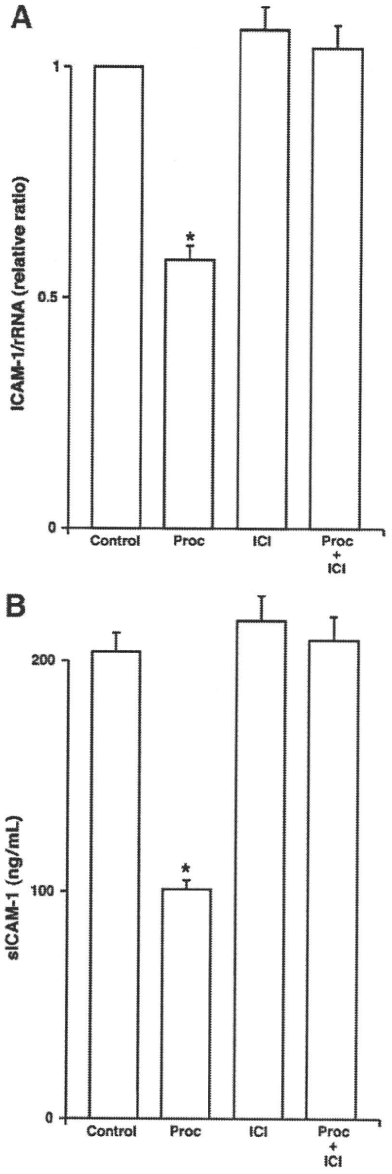

Fig. 5. (A) The expression of ICAM-1 mRNA before type 14 rhinovirus infection in human tracheal epithelial cells treated with procaterol (0.1 μM, 72 h, Proc), a vehicle of procaterol (0.01% ethanol, Control), ICI 118551 (1 μM, ICI), or procaterol plus ICI 118551 (Proc + ICI) detected by real-time quantitative RT-PCR. The epithelial cells isolated from the same donors were treated with either procaterol, vehicle, ICI 118551, or procaterol plus ICI 118551. ICAM-1 mRNA was normalized to the constitutive expression of ribosomal RNA (rRNA). The expression of ICAM-1 mRNA in the cells treated with vehicle (Control) was set to 1.0. Results are means ± S.E.M. from five different tracheae (2 ex-smokers and 3 non-smokers). Significant differences from control values are indicated by $^*P<0.05$. (B) The sICAM-1 concentrations in supernatant fluids before type 14 rhinovirus infection in human tracheal epithelial cells treated with procaterol (0.1 μM, 72 h Proc), the vehicle of procaterol (0.01% ethanol, Control), ICI 118551 (1 μM, ICI), or procaterol plus ICI 118551 (Proc + ICI) detected by enzyme immunoassay. The concentrations of sICAM-1 in the supernatant fluids are expressed as ng/ml. Results are means ± S.E.M. from five different tracheae (2 ex-smokers and 3 non-smokers). Significant differences from control values are indicated by $^*P<0.05$.

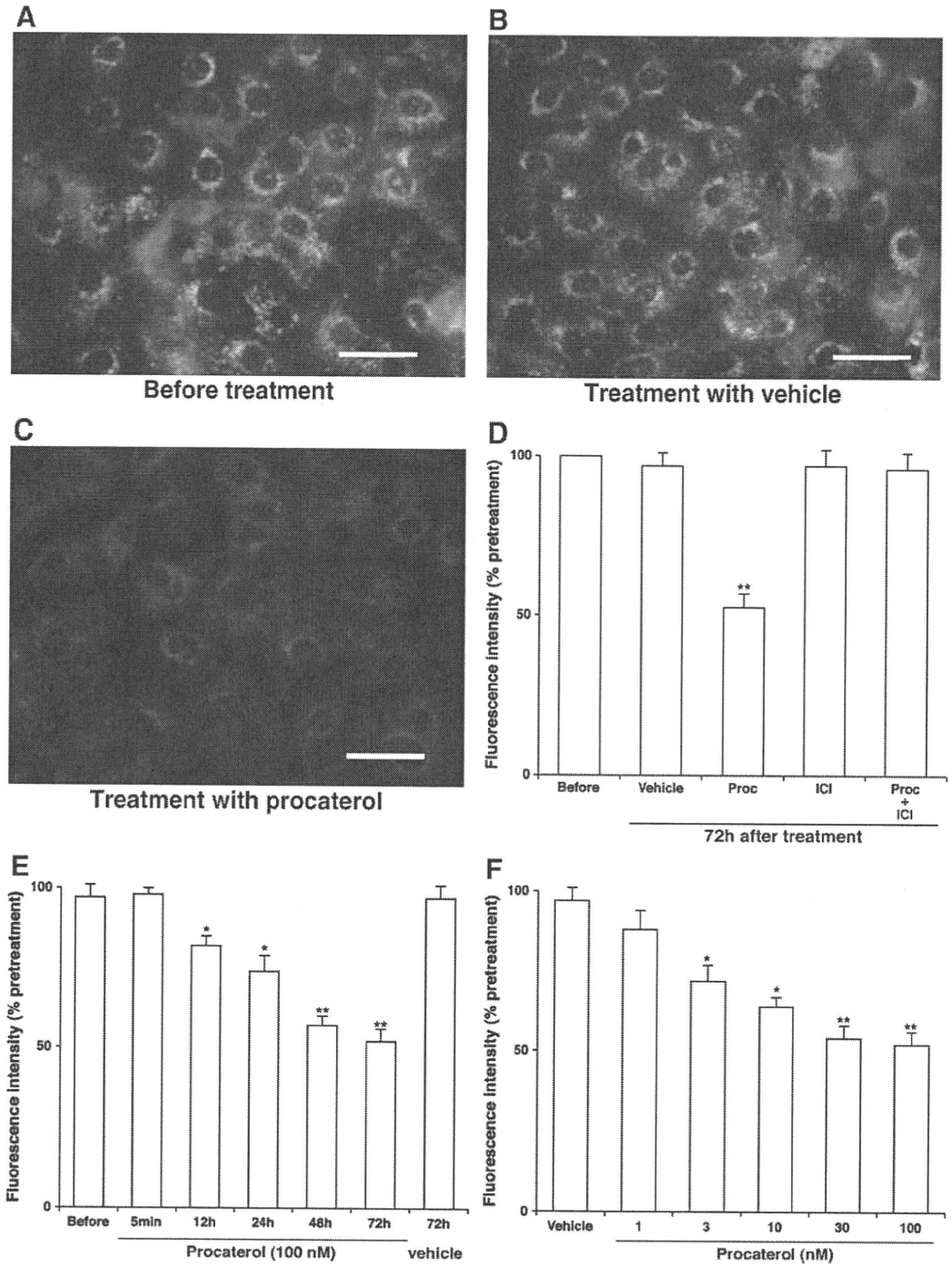

Fig. 6. (A–C) Changes in the distribution of acidic endosomes with green fluorescence in human tracheal epithelial cells before (A) and 3 days (72 h) after treatment with procaterol (0.1 μM) (C) or the vehicle of procaterol (0.01% ethanol) (B). Data are representative of five different experiments (2 ex-smokers and 3 non-smokers). (Bar = 100 μm). (D) The fluorescence intensity of acidic endosomes before and 3 days (72 h) after treatment with procaterol (0.1 μM, Proc), ICI 118551 (1 μM, ICI), or procaterol plus ICI 118551 (Proc + ICI), or the vehicle of procaterol (0.01% ethanol, Vehicle). Results are expressed as relative fluorescence intensity (%) compared with that before any treatment (Before) and reported as means ± S.E.M. from five samples (2 ex-smokers and 3 non-smokers). Significant differences from values before any treatment (Before) are indicated by $^{**}P<0.01$. (E) Time course of the effects of procaterol (0.1 μM) on the fluorescence intensity of acidic endosomes in the cells treated for times ranging from 0 (Before) to 3 days (72 h) and the fluorescence intensity in the cells treated with vehicle (0.01% ethanol, vehicle) for 3 days (72 h). Results are means ± S.E.M. from five different tracheae (2 ex-smokers and 3 non-smokers). Significant differences from before any treatment (Before) are indicated by $^{*}P<0.05$ and $^{**}P<0.01$. (F) Dose-response effects of procaterol on the fluorescence intensity of acidic endosomes 3 days (72 h) after treatment. The cells were treated with procaterol or the vehicle (0.01% ethanol, Vehicle) for 3 days (72 h). Results are means ± S.E.M. from five different tracheae (2 ex-smokers and 3 non-smokers). Significant differences from vehicle alone (Vehicle) are indicated by $^{*}P<0.05$ and $^{**}P<0.01$.

Treatment of the cells with ICI 118551 (1 μM, 72 h) reversed the inhibitory effects of procaterol on the baseline and rhinovirus infection-induced secretion of interleukin-1β, interleukin-6, and interleukin-8 (Fig. 7), whereas ICI 118551 alone did not change the secretion of these cytokines (data not shown).

In contrast, ultraviolet-irradiated type 14 rhinovirus did not increase interleukin-1β, interleukin-6, and interleukin-8 at any time after infection (Fig. 7). Secretion of interleukin-1β, interleukin-6, and interleukin-8 in supernatant fluids of the cells from three ex-smokers did not differ from those of three patients who had never smoked

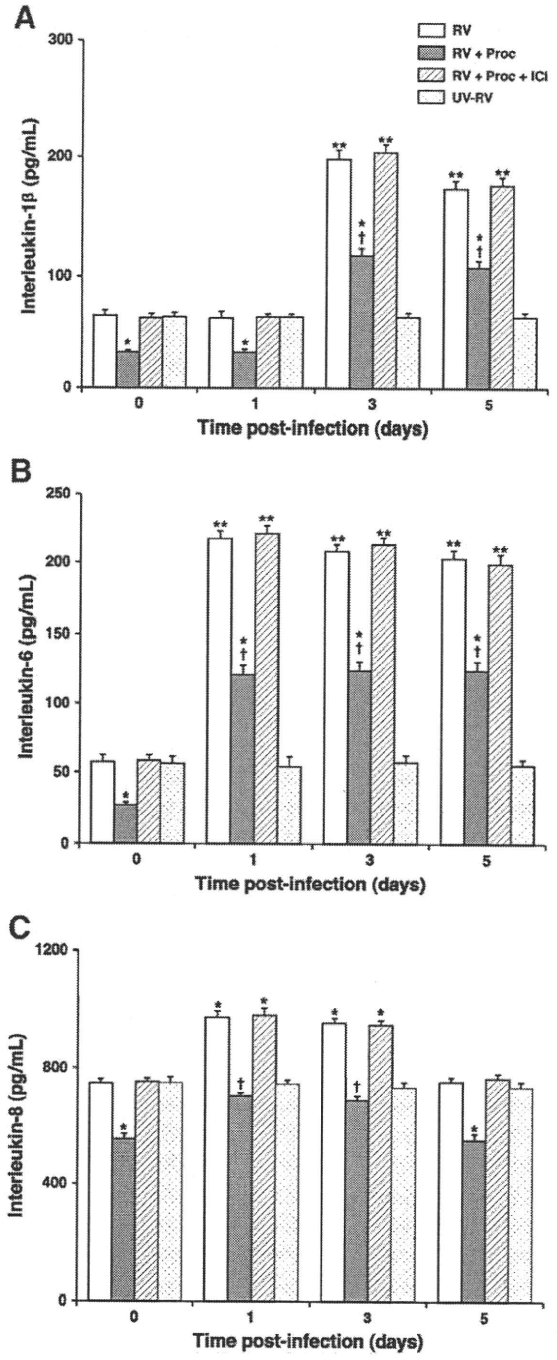

Fig. 7. (A–C) Time course changes in the release of cytokines into supernatant fluids of human tracheal epithelial cells before and after type 14 rhinovirus infection in the presence of procaterol (0.1 μM, RV + Proc), procaterol (0.1 μM) plus ICI 118551 (1 μM) (RV + Proc + ICI), or the vehicle of procaterol (0.01% ethanol, RV) and after UV-inactivated RV14 infection (UV–RV). The epithelial cells isolated from the same donors were treated with either procaterol, vehicle, or procaterol plus ICI 118551. The concentrations of cytokines in the supernatant fluids are expressed as pg/ml. Results are means ± S.E.M. from six different tracheae (3 ex-smokers and 3 non-smokers). Significant differences from values before type 14 rhinovirus infection (time 0) in the presence of vehicle of procaterol (0.01% ethanol) are indicated by $^{*}P<0.05$ and $^{**}P<0.01$. Significant differences from type 14 rhinovirus infection alone (RV) at each time after infection are indicated by $+P<0.05$.

(data not shown). Likewise, secretion of interleukin-1β, interleukin-6, and interleukin-8 in supernatant fluids of the cells from three patients complicated with COPD did not differ from those from 30 patients without COPD complications (data not shown).

3.7. Effects on NF-kappa B

Procaterol (0.1 μM, 72 h) significantly reduced the amount of p50, p65, and c-Rel of NF-κB in the nuclear extracts in the cells before type 14 rhinovirus infection (Fig. 8A–C). On the other hand, the amount of p50, p65, and c-Rel of NF-κB in the nuclear extracts increased at 2 h after type 14 rhinovirus infection (Fig. 8A–C), and procaterol (0.1 μM) also significantly reduced the amount of p50, p65, and c-Rel of NF-κB induced by type 14 rhinovirus infection (Fig. 8A–C). Furthermore, ICI 118551 (1 μM) reversed the inhibitory effects of procaterol on the NF-κB activation before (data not shown) and after type 14 rhinovirus infection (Fig. 8A–C), whereas ICI 118551 alone did not change the NF-κB activation before the infection (Fig. 8A–C).

Type 14 rhinovirus infection increased the cytosolic amount of p-IκB-α 2 h after infection, and procaterol (0.1 μM, 72 h) significantly decreased the amount of p-IκB-α induced by the infection (Fig. 9A and B). Furthermore, ICI 118551 (1 μM, 72 h) reversed the effects of procaterol on the p-IκB-α after type 14 rhinovirus infection (Fig. 9A and B). In contrast, before type 14 rhinovirus infection, neither procaterol (0.1 μM, 72 h), ICI 118551 (1 μM, 72 h), nor procaterol plus ICI 118551 had any effect on p-IκB-α in the cellular proteins.

On the other hand, type 14 rhinovirus infection decreased the cytosolic amount of IκB-α 2 h after infection, and procaterol (0.1 μM, 72 h) significantly increased the amount of IκB-α after the infection (Fig. 9A and C). Furthermore, ICI 118551 (1 μM) reversed the effects of procaterol on the IκB-α after the infection (Fig. 9A and C). In contrast, before type 14 rhinovirus infection, neither procaterol (0.1 μM, 72 h), ICI 118551 (1 μM, 72 h) nor procaterol plus ICI 118551 had any effect on the IκB-α in the cellular proteins (Fig. 9A and C).

3.8. Effects on intracellular cAMP

Significant intracellular cAMP levels were detected in the cells before any treatment (44.0 ± 4.2 pmol/mg protein, n = 5) (Fig. 10A). Treatment of the cells with procaterol (0.1 μM) increased intracellular cAMP at 10 min and 20 min after the addition of procaterol, and increased levels of intracellular cAMP were still observed at 3 days (72 h) after the addition of procaterol (Fig. 10A).

Treatment with the vehicle alone (0.01% ethanol) for 20 min did not change intracellular cAMP levels (Fig. 10B). ICI 118551 (1 μM, 20 min) alone did not change the intracellular cAMP levels, while ICI 118551 reversed the effects of procaterol (0.1 μM, 20 min) on intracellular cAMP to the levels in the cells treated with vehicle (Fig. 10B). Intracellular cAMP levels in the cells treated with procaterol (0.1 μM) plus ICI 118551 for 20 min were significantly lower than those in the cells treated with procaterol alone (Fig. 10B). Treatment with ICI 118551 for 10 min or 3 days (72 h) also reversed the effects of procaterol (0.1 μM) on intracellular cAMP to the levels in the cells treated with the vehicle (data not shown).

4. Discussion

In the present study, we have shown that a β_2 agonist, procaterol hydrochloride, reduced the titers of a major group rhinovirus, type 14 rhinovirus, in supernatant fluids and RNA replication of the virus in the primary cultures of human tracheal epithelial cells. Pretreatment with procaterol reduced the expression of mRNA and protein of ICAM-1, the receptor for the major group of rhinoviruses (Greve et al., 1989) before rhinovirus infection. The minimum dose of type 14 rhinovirus necessary to cause infection in the cells treated with procaterol was significantly higher than that in the cells treated with the vehicle of procaterol. A selective β_2-adrenergic receptor antagonist ICI 118551 reversed the inhibitory effects of procaterol on type 14 rhinovirus titer levels, RNA replication of the virus, the expression of mRNA and protein of ICAM-1, and NF-κB. Treatment of the cells with ICI 118551 also reversed the inhibitory effects of procaterol on the susceptibility

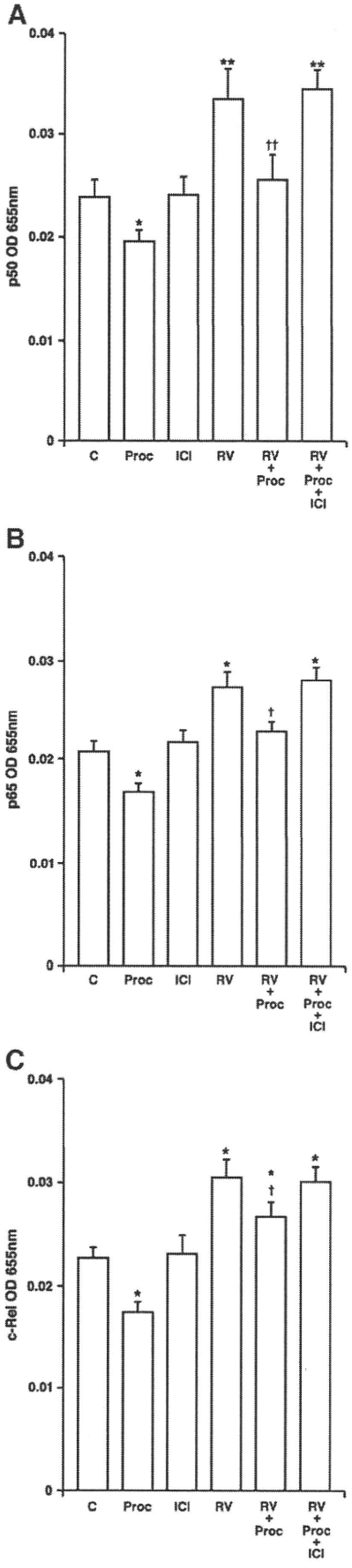

of the cells to type 14 rhinovirus infection. These findings suggest that β_2-adrenoceptor-mediated effects of procaterol might inhibit type 14 rhinovirus infection partly through reducing the production of its receptor, ICAM-1.

Furthermore, treatment with procaterol reduced the number and fluorescence intensity of acidic endosomes from which rhinovirus RNA enters into the cytoplasm (Casasnovas and Springer, 1994; Turner and Couch, 2006), dose- and time-dependently, and ICI 118551 reversed the inhibitory effects of procaterol on the acidic endosomes. If only ICAM-1 expression is reduced on the cells, a similar amount of virus will be produced and released into supernatant fluids, and viral titers of procaterol-treated cells will reach to those of control cells after long periods of culture. On the other hand, in this study, procaterol also reduced the number of acidic endosomes where virus RNA enters into the cytoplasm. Therefore, by the reduction of acidic endosomes, inhibition of RNA entry into the cytoplasm might reduce the number of virus virions that enter into the cytoplasm, and viral titers of procaterol-treated cells did not reach control cells after long periods of culture. Procaterol might also inhibit type 14 rhinovirus infection partly through inhibiting rhinovirus RNA entry from acidic endosomes into the cells.

Treatment of the cells with procaterol significantly decreased the viral titers of type 14 rhinovirus in supernatant fluids from 12 h after infection. Procaterol also decreased the type 14 rhinovirus RNA at 1 day (24 h) and at 3 days (72 h) after infection. In contrast, there is no difference in the rate of increase in viral titers between rhinovirus infected control cells and procaterol-treated cells. These results suggest that procaterol may affect the ability of rhinovirus to infect cells and possibly does not affect the rate of rhinovirus replication once within the cell.

Likewise, to examine the susceptibility to type 14 rhinovirus infection, the epithelial cells were treated with procaterol from 3 days (72 h) before infection with type 14 rhinovirus until the end of the infection. The epithelial cells were exposed to serial 10-fold dilutions of type 14 rhinovirus at a dose ranging from 10^1 to 10^5 $TCID_{50}$ units/ml of type 14 rhinovirus containing procaterol. After exposure to type 14 rhinovirus, cells were rinsed with PBS, and fresh medium without addition of procaterol was replaced. Cells in the tubes were then cultured. Therefore, in this experiment, we studied the effects of procaterol on the ability of type 14 rhinovirus to infect. In contrast, cells were treated with procaterol before and during type 14 rhinovirus infection but were not treated with procaterol after infection. Therefore, the minimum dose of type 14 rhinovirus necessary to cause infection might not explain the ability of type 14 rhinovirus to replicate within the cell.

Human embryonic fibroblast cells did not show any morphological change that demonstrates the presence of type 14 rhinovirus when supernatant fluids collected 1 h after infection were added to the fibroblast cells. In contrast, supernatant fluids 12 h after infection produced morphological change on the cells showing the presence of rhinovirus (Condit, 2006; Numazaki et al., 1987). These findings suggest that supernatant fluids 12 h after infection contained significant amounts of type 14 rhinovirus virions that were newly produced after infection.

Fig. 8. (A-C) Amount of p50 (A), p65 (B), and c-Rel (C) in nuclear extracts in human tracheal epithelial cells treated with procaterol (0.1 μM, Proc), vehicle (0.01% ethanol, C), or ICI 118551 (1 μM) (ICI) for 3 days (72 h) before type 14 rhinovirus infection, and the amount of p50, p65, and c-Rel in the cells 2 h after infection with type 14 rhinovirus in the presence of procaterol (RV + Proc), in the presence of the vehicle of procaterol (0.01% ethanol, RV), or the presence of procaterol plus ICI 118551 (RV + Proc + ICI) from 3 days (72 h) before rhinovirus infection until the end of the experiments after rhinovirus infection. Results are expressed as OD, and are means ± S.E.M. from five different tracheae (2 ex-smokers and 3 non-smokers). Significant differences from control values (C) before rhinovirus infection are indicated by $^*P<0.05$ and $^{**}P<0.01$. Significant differences from rhinovirus infection alone (RV) are indicated by $+P<0.05$ and $++P<0.01$.

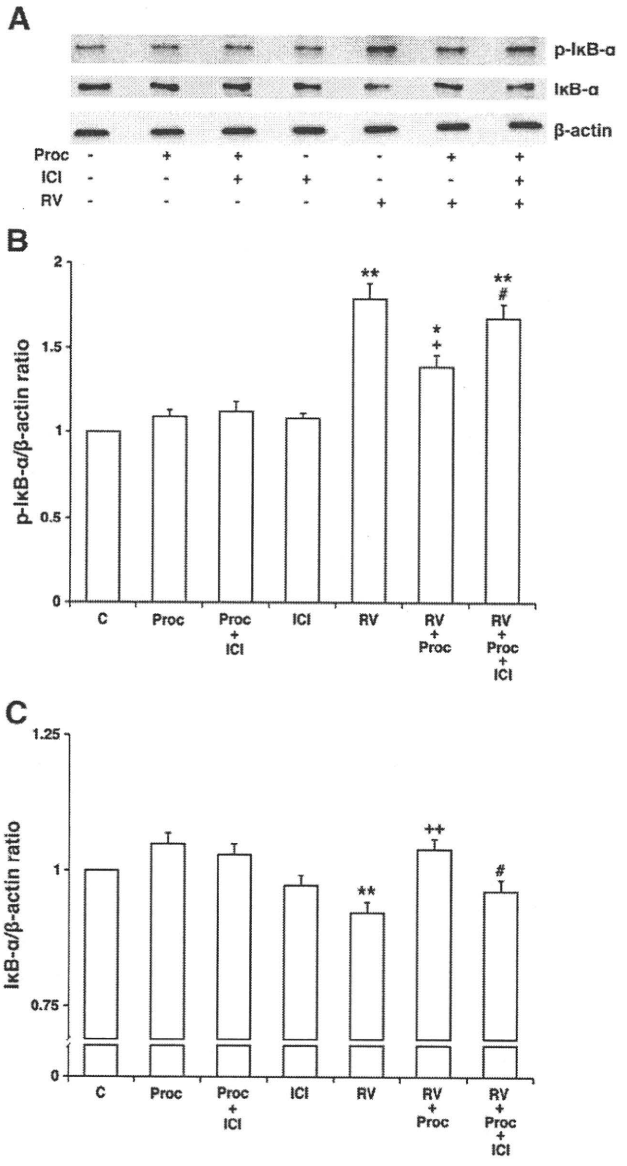

Fig. 9. (A) Cytosolic amount of p-IκB-α, IκB-α or β-actin in human tracheal epithelial cells before and 2 h after type 14 rhinovirus infection (RV) in the presence of procaterol (0.1 μM, Proc) or ICI 118551 (1 μM, ICI) for 3 days (72 h). The data are representative of three different experiments (2 ex-smokers and 1 non-smoker). (B and C) Cytosolic amount of p-IκB-α (B) and IκB-α (C) in the cells treated with procaterol (0.1 μM, Proc), procaterol plus ICI 118551 (1 μM) (Proc + ICI), ICI 118551 (ICI), or vehicle (0.01% ethanol, C) for 3 days (72 h) before type 14 rhinovirus infection and the amount in the cells 2 h after infection with type 14 rhinovirus in the presence of procaterol (RV + Proc), the presence of the vehicle of procaterol (0.01% ethanol, RV), or the presence of procaterol plus ICI 118551 (RV + Proc + ICI) from 3 days (72 h) before rhinovirus infection until the end of the experiments after rhinovirus infection. The data were obtained by dividing the results in each culture condition by the results of β-actin. The cytosolic amount of p-IκB-α and IκB-α in the cells treated with vehicle before rhinovirus infection (0.01% ethanol, C) was set to 1.0. Significant differences from control values (C) before rhinovirus infection are indicated by $^{*}P<0.05$ and $^{**}P<0.01$. Significant differences from rhinovirus infection alone (RV) are indicated by $+P<0.05$ and $++$ $P<0.01$. Significant differences from rhinovirus infection in the presence of procaterol (RV + Proc) are indicated by # $P<0.05$.

Furthermore, in the tracheal cells from all subjects which cells were infected with rhinovirus, the supernatant fluids collected during 1 day (24 h) to 3 days (72 h) after infection contained consistent levels of type 14 rhinovirus. These findings suggest that human tracheal epithelial cells from all subjects were constantly infected with type 14 rhinoviruses.

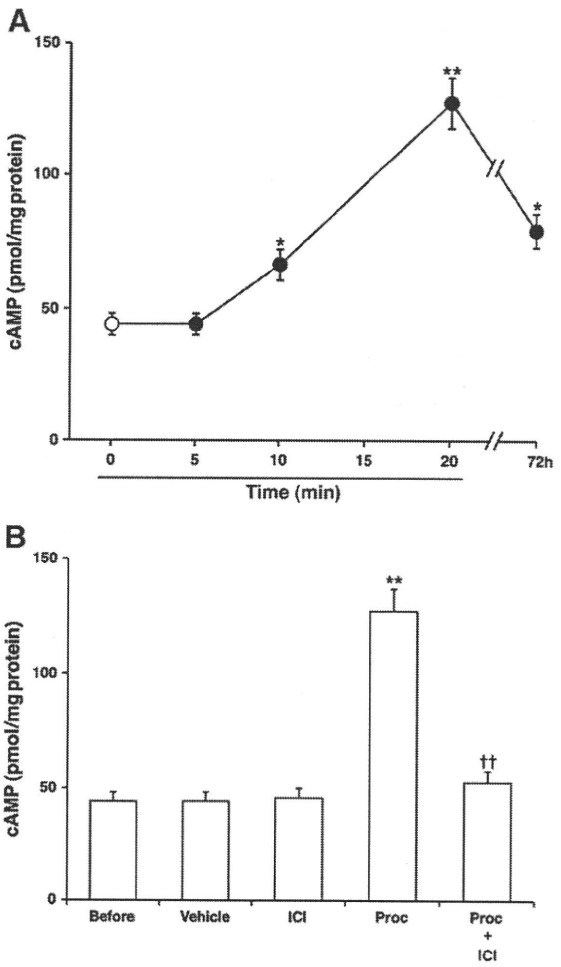

Fig. 10. (A) Intracellular concentrations of cAMP in human tracheal epithelial cells before (time 0, open circle), 5 min, 10 min, 20 min, and 3 days (72 h) after treatment with procaterol (0.1 μM, closed circles). Results are expressed as pmol/mg protein, and are means ± S.E.M. from five different tracheae (2 ex-smokers and 3 non-smokers). Significant differences from control values before treatment (time 0) are indicated by $^{*}P<0.05$ and $^{**}P<0.01$. (B) Intracellular concentrations of cAMP in human tracheal epithelial cells before (Before) and 20 min after treatment with either procaterol (0.1 μM, Proc), ICI 118551 (1 μM, ICI), procaterol (0.1 μM) plus ICI 118551 (1 μM) (Proc + ICI), or vehicle (0.01% ethanol, Vehicle). The epithelial cells isolated from the same donors were treated with either procaterol, vehicle, ICI 118551, or procaterol plus ICI 118551. Results are expressed as pmol/mg protein and are means ± S.E.M. from five different tracheae (2 ex-smokers and 3 non-smokers). Significant differences from control values before treatment (Before) are indicated by $^{**}P<0.01$. Significant differences from procaterol (Proc) are indicated by $++P<0.01$.

The major group of rhinoviruses enters the cytoplasm of infected cells after binding to its receptor ICAM-1 (Greve et al., 1989). In the present study, procaterol reduced ICAM-1 expression in the primary cultures of human tracheal epithelial cells. On the other hand, a β_2 agonist, fenoterol, reduces ICAM-1 expression in the human bronchial epithelial cells (Oddera et al., 1998), and salmeterol and procaterol reduce ICAM-1 expression in fibroblast cells (Silvestri et al., 2001; Yoshida et al., 2009). The results of reduced ICAM-1 expression observed in this study are consistent with the results of these reports. The inhibitory effects of procaterol on ICAM-1 expression in human tracheal epithelial cells might be associated with the inhibitory effects of procaterol on type 14 rhinovirus infection, as previously reported on the inhibitory effects of agents including dexamethasone, erythromycin, a proton pump inhibitor (lansoprazole), and a Japanese herbal medicine (Hochu-ekki-to) (Sasaki et al., 2005; Suzuki et al., 2000, 2002; Yamaya et al., 2007).

The endosomal pH is suggested to be regulated by vacuolar H^+-ATPase (Mellman et al., 1986) and by ion transport across the Na^+/H^+

exchangers (Marshansky and Vinay, 1996; Nass and Rao, 1998). A vacuolar H^+-ATPase inhibitor bafilomycin, an inhibitor of Na^+/H^+ exchangers 5-(N-ethyl-N-isopropyl) amiloride (EIPA) and N″-[3-(Hydroxymethyl)-5-(1 H-pyrrol-1-yl) benzoyl] guanidine methonesulfonate (FR168888) increase endosomal pH and inhibit type 14 rhinovirus infection in cultured human tracheal epithelial cells (Suzuki et al., 2001). In the present study, procaterol increased the endosomal pH, although we have no data with which to determine whether procaterol inhibits vacuolar H^+-ATPase or Na^+/H^+ exchangers. On the other hand, the addition of cyclic AMP (cAMP) increases endosomal pH in kidney epithelial cells through the inhibition of a Na^+/H^+ exchanger (Gekle et al., 2002), and procaterol increases cAMP levels in airway epithelial cells as shown in a previous report (Koyama et al., 1999) and in this study. In contrast, cAMP alone has no effect on vacuolar H^+-ATPase activities in Madin–Darby canine kidney cells, but has synergic action on vacuolar H^+-ATPase activation induced by arginine vasopressin (Oliveira-Souza et al., 2004). These findings suggest the possibility that procaterol has an inhibitory effect on Na^+/H^+ exchanger through the increased production of cAMP in airway epithelial cells.

ICAM-1 also plays a vital role in the recruitment and migration of immune effector cells to sites of local inflammation observed in patients with bronchial asthma and COPD (Grunberg and Sterk, 1999; Riise et al., 1994). The inhibitory effects of β_2 agonists on ICAM-1, as shown in the previous reports and in this study, may also be associated with the inhibition of airway inflammation and subsequently occurring exacerbations of bronchial asthma and COPD (Barnes, 2007; Calverley et al., 2007) after rhinoviruses infection.

Rhinoviruses are associated with exacerbations of bronchial asthma (Johnston et al., 1995) and COPD (Seemungal et al., 2000). Neutrophilic and eosinophilc inflammation in the exacerbations of bronchial asthma and COPD are suggested to be associated with a variety of mediators including interleukin-6 and interleukin-8 by rhinovirus infection (Pizzichini et al., 1998; Seemungal et al., 2000). Procaterol reduces the number of eosinophils in bronchoalveolar lavage fluids in mice after ovalbumin challenge (Tashimo et al., 2007) and inhibits interleukin-1β- and tumor necrosis factor (TNF)-α-mediated eosinophil chemotactic activity (Koyama et al., 1999). β_2 Agonists may also modulate eosinophil-related inflammation in bronchial asthma. Furthermore, in the present study, procaterol reduced type 14 rhinovirus infection-induced production of interleukin-1β, interleukin-6, and interleukin-8, and ICI 118551 reversed the inhibitory effects of procaterol on the release of these interleukins. These findings are consistent with previous findings showing the inhibitory effects of procaterol on plasma levels of cytokines including interleukin-1β in rats (Izeboud et al., 2004), and the inhibitory effects of salmeterol on the production of pro-inflammatory cytokines and monokines including RANTES (regulated on activation, normal T cells expressed and secreted/CCL5) in primary culture of normal bronchial epithelial cells after rhinovirus infection (Edwards et al., 2006). Similar to the inhibitory effects of a glucocorticoid (Suzuki et al., 2000), procaterol may also modulate airway inflammation induced by rhinovirus infections.

NF-κB increases the expression of genes for ICAM-1 and various pro-inflammatory cytokines (Papi and Johnston, 1999; Zhu et al., 1996). In the present study, procaterol reduced the expression of ICAM-1 before rhinovirus infection and the secretion of pro-inflammatory cytokines in supernatant fluids before and after rhinovirus infection. Rhinovirus infection increased activation of NF-κB as previously reported (Suzuki et al., 2002). Rhinovirus increased p50, p65, and c-Rel of NF-κB in the nuclear extracts, increased the cytosolic quantity of p-IκB-α, and decreased the cytosolic quantity of IκB-α. Procaterol reduced p50, p65, and c-Rel of NF-κB induced by rhinovirus infection as well as baseline NF-κB before rhinovirus infection. Procaterol also reduced p-IκB-α and increased IκB-α in the cellular proteins after rhinovirus infection, although procaterol had no effect on p-IκB-α and IκB-α in the cellular proteins before rhinovirus infection. The inhibitory effects of procaterol on NF-κB activation observed in this study are consistent with those of salmeterol in lung myofibroblasts (Baouz et al., 2005). Furthermore, a selective β_2-adrenergic receptor antagonist, ICI 118551, reversed the inhibitory effects of procaterol on the activation of NF-κB in the nuclear extracts before and after type 14 rhinovirus infection. ICI 118551 also reversed the effects of procaterol on p-IκB-α and IκB-α in the cellular proteins after rhinovirus infection. These findings suggest that procaterol might reduce the expression of ICAM-1 on the cells and secretion of pro-inflammatory cytokines partly through the reduction of NF-κB activation.

In contrast, Edwards et al. reported that salmeterol increases interleukin-6 production and enhances NF-kB pathway activation following rhinovirus infection in bronchial epithelial cell line (BEAS-2B) cells and primary cultures of normal bronchial epithelial cells (2007). Furthermore, another report demonstrated that β_2 agonists, treated for 30 min before stimulation with interleukin-1β do not affect NF-kB-induced activation of the interleukin-6 gene in airway smooth muscle cells (Kaur et al., 2008). On the other hand, production of interleukin-6 after rhinovirus infection through the activation of NF-κB has been reported in A549 alveolar epithelial type II-like cells (Zhu et al., 1996). Fragaki et al. demonstrated that salmeterol plus corticosteroid reduced interleukin-6 release in response to *Staphylococcus aureus* from transformed human tracheal gland cell line partly through the inhibition of NF-kB (2006). Inhibition of NF-κB and TNF-α-induced interleukin-6 production by salmeterol was also reported in lung myofibroblasts (Baouz et al., 2005). We previously reported that reduced production of interleukin-6 by a macrolide antibiotic erythromycin and a mucolytic agent L-carbocisteine is associated with the inhibition of NF-κB (Suzuki et al., 2002; Yasuda et al., 2006). Thus, these findings suggest that different effects of β_2 agonists on interleukin-6 and NF-κB after rhinovirus infection or after addition of stimulants may be partly associated with differences in cell type and with culture condition. However, the precise mechanisms are uncertain.

In this study, procaterol reduced viral titers and cytokine concentration in the supernatant fluids. It also decreased viral RNA replication, ICAM-1 expression, acidic endosomes, and NF-κB activation in the cells. Procaterol decreased susceptibility of the cells to virus infection and increased intracellular cAMP. The levels of intracellular cAMP induced by procaterol in this study were consistent with those reported previously (Koyama et al., 1999). On the other hand, a selective β_2-adrenergic receptor antagonist ICI 118551 reversed the inhibitory effects of procaterol on various cell functions and reduced cellular cAMP concentrations stimulated by procaterol. These findings suggest that the effects of procaterol observed in this study might be mediated by the β_2-adrenergic receptor.

Procaterol alone did not change cell viability, including cell number, assessed by the exclusion of trypan blue, and LDH concentrations in supernatant fluids. However, procaterol reduced NF-κB activation before and after RV infection. These findings suggest that reduced cytokine release might be partly associated with the inhibition of NF-κB activation but not with cell injury.

In the present study, type 14 rhinovirus titers in supernatant fluids in the cells from three patients with COPD did not differ from those in the cells from 35 patients without COPD complications. Epidermal growth factor receptor, which is up-regulated in COPD (O'Donnell et al., 2004), is associated with ICAM-1 and interleukin-8 production in airway epithelial cells, although we did not examine the production of epidermal growth factor receptor in the epithelial cells in this study. On the other hand, deficient induction of interferon-gamma (IFN-γ)-mediated high rhinovirus RNA replication was reported in the bronchial epithelial cells from patients with bronchial asthma (Contoli et al., 2006), but no patients were complicated with bronchial asthma in this study. We observed no significant mRNA expression of IFN-γ in the human tracheal epithelial cells from patients with or

without COPD complication (data not shown). Because we isolated the cells from human tracheae after death, the conditions before death, at the time of death, and the conditions from the time of death to cell isolation might also mask the characteristic features of cultured cell function. However, further studies are needed to clarify the difference of the magnitude of rhinovirus replication in the cells from COPD patients.

Likewise, the amount of cytokine release after rhinovirus infection did not differ between smokers and non-smokers. Conditions before death, at the time of death, and the conditions from the time of death to the cell isolation may also mask the cell condition including different response to beta agonists in smokers. The precise reason is uncertain.

Baseline levels for all cytokines observed in this study were higher than those in other studies including those by Edwards et al. (2007), while baseline levels in this study were consistent with those reported previously by us (Yamaya et al., 2007). Although the precise reason is uncertain, human bronchial epithelial cells in the study by Edwards were cultured in BEBM medium, and human tracheal epithelial cells in this study were cultured in Dulbecco's modified Eagle's Medium (DMEM)-Ham's F-12 medium (50/50, vol/vol) containing 2% USG. As previously reported (Yamaya et al., 1992), differences in the factors in culture medium may change cell functions including ion transport and protein production. Differences in culture medium may be partly associated with baseline levels of cytokines.

In summary, this is the first report that a β_2 agonist procaterol reduces type 14 rhinovirus titers in supernatant fluids, reduced rhinovirus RNA replication in cultured human tracheal epithelial cells, and decreases the susceptibility of the cells to rhinovirus infection. This may occur partly through the reduced expression of ICAM-1, the receptor for the major group of rhinoviruses, and reduction in the number of acidic endosomes from which rhinovirus RNA enters into the cytoplasm. Procaterol reduced baseline and rhinovirus infection-induced release of interleukin-1β, interleukin-6, and interleukin-8 in supernatant fluids. Procaterol may inhibit the infection of the major group of rhinoviruses and modulate the inflammatory responses in the airways after rhinovirus infection.

Conflict of interest

None.

Acknowledgments

The authors thank Mr. Grant Crittenden for reading the manuscript.

This study was supported by the Health and Labour Sciences Research Grants for Research on Measures for Intractable Diseases from the Ministry of Health, Labour and Welfare of the Japanese government (H20 nanchi ippann 035), by a grant to the Respiratory Failure Research Group from the Ministry of Health, Labour and Welfare of the Japanese government, and supported by Ohtsuka Pharmaceutical Co. Ltd.

References

Akira, S., Hirano, T., Taga, T., Kishimoto, T., 1990. Biology of multifunctional cytokines: IL 6 and related molecules (IL 1 and TNF). FASEB J. 4, 2860–2867.

Baouz, S., Giron-Michel, J., Azzarone, B., Giuliani, M., Cagnoni, F., Olsson, S., Testi, R., Gabbiani, G., Walter, G., Canonica, G.W., 2005. Lung myofibroblasts as targets of salmeterol and fluticasone propionate: inhibition of α-SMA and NF-kappaB. Int. Immunol. 17, 1473–1481.

Barnes, P.J., 2007. Scientific rationale for using a single inhaler for asthma control. Eur. Respir. J. 29, 587–595.

Bilski, A.J., Halliday, S.E., Fitzgerald, J.D., Wale, J.L., 1983. The pharmacology of a β2-selective adrenoceptor antagonist (ICI 118, 551). J. Cardiovasc. Pharmacol. 5, 430–437.

Calverley, P.M., Anderson, J.A., Celli, B., Ferguson, G.T., Jenkins, C., Jones, P.W., Yates, J.C., Vestbo, J., TORCH investigators, 2007. Salmeterol and fluticasone propionate and survival in chronic obstructive pulmonary disease. N. Engl. J. Med. 356, 775–789.

Casasnovas, J.M., Springer, T.A., 1994. Pathway of rhinovirus disruption by soluble intercellular adhesion molecule 1 (ICAM-1): an intermediate in which ICAM-1 is bound and RNA is released. J. Virol. 68, 5882–5889.

Chiulli, A.C., Trompeter, K., Palmer, M., 2000. A novel high throughput chemiluminescent assay for measurement of cellular cyclic adenosine monophosphate levels. J. Biomol. Screen. 5, 239–247.

Condit, R.C., 2006. Principles of virology, In: Knipe, D.M., Howley, P.M. (Eds.), Fields Virology, 5th ed. Lippincott Williams and Wilkins, Philadelphia, PA, pp. 25–57.

Contoli, M., Message, S.D., Laza-Stanca, V., Edwards, M.R., Wark, P.A., Bartlett, N.W., Kebadze, T., Mallia, P., Stanciu, L.A., Parker, H.L., Slater, L., Lewis-Antes, A., Kon, O.M., Holgate, S.T., Davies, D.E., Kotenko, S.V., Papi, A., Johnston, S.L., 2006. Role of deficient type III interferon-λ production in asthma exacerbations. Nat. Med. 12, 1023–1026.

Edwards, M.R., Johnson, M.W., Johnston, S.L., 2006. Combination therapy: synergistic suppression of virus-induced chemokines in airway epithelial cells. Am. J. Respir. Cell Mol. Biol. 34, 616–624.

Edwards, M.R., Haas, J., Panettieri Jr., R.A., Johnson, M., Johnston, S.L., 2007. Corticosteroids and β_2 agonists differentially regulate rhinovirus-induced interleukin-6 via distinct cis-acting elements. J. Biol. Chem. 282, 15366–15375.

Fiorucci, S., Antonelli, E., Distrutti, E., Del Soldato, P., Flower, R.J., Clark, M.J., Morelli, A., Perretti, M., Ignarro, L.J., 2002. NCX-1015, a nitric-oxide derivative of prednisolone, enhances regulatory T cells in the lamina propria and protects against 2, 4, 6-trinitrobenzene sulfonic acid-induced colitis in mice. Proc. Natl. Acad. Sci. U. S. A. 99, 15770–15775.

Fragaki, K., Kileztky, C., Trentesaux, C., Zahm, J.M., Bajolet, O., Johnson, M., Puchelle, E., 2006. Downregulation by a long-acting β_2-adrenergic receptor agonist and corticosteroid of *Staphylococcus aureus*-induced airway inflammatory mediator production. Am. J. Physiol. 291, L11–L18.

Gekle, M., Serrano, O.K., Drumm, K., Mildenberger, S., Freudinger, R., Gassner, B., Jansen, H.W., Christensen, E.I., 2002. NHE3 serves as a molecular tool for cAMP-mediated regulation of receptor-mediated endocytosis. Am. J. Physiol. 283, F549–F558.

Greve, J.M., Davis, G., Meyer, A.M., Forte, C.P., Yost, S.C., Marlor, C.W., Kamarck, M.E., McClelland, A., 1989. The major human rhinovirus receptor is ICAM-1. Cell 56, 839–847.

Grunberg, K., Sterk, P.J., 1999. Rhinovirus infections: induction and modulation of airways inflammation in asthma. Clin. Exp. Allergy 29 (Suppl 2), 65–73.

Izeboud, C.A., Hoebe, K.H., Grootendorst, A.F., Nijmeijer, S.M., van Miert, A.S., Witkamp, R.R., Rodenburg, R.J., 2004. Endotoxin-induced liver damage in rats is minimized by β_2-adrenoceptor stimulation. Inflamm. Res. 53, 93–99.

Johnson, M., 1991. Salmeterol: a novel drug for the treatment of asthma. Agents Actions Suppl. 34, 79–95.

Johnston, S.L., Pattemore, P.K., Sanderson, G., Smith, S., Lampe, F., Josephs, L., Symington, P., O'Toole, S., Myint, S.H., Tyrrell, D.A.J., Holgate, S.T., 1995. Community study of role of viral infections in exacerbations of asthma in 9-11 year old children. Br. Med. J. 310, 1225–1229.

Kaur, M., Holden, N.S., Wilson, S.M., Sukkar, M.B., Chung, K.F., Barnes, P.J., Newton, R., Giembycz, M.A., 2008. Effect of β_2-adrenoceptor agonists and other cAMP-elevating agents on inflammatory gene expression in human ASM cells: a role for protein kinase A. Am. J. Physiol. 295, L505–L514.

Kim, J.Y., Park, S.J., Yun, K.J., Cho, Y.W., Park, H.J., Lee, K.T., 2008. Isoliquiritigenin isolated from the roots of *Glycyrrhiza uralensis* inhibits LPS-induced iNOS and COX-2 expression via the attenuation of NF-kappaB in RAW 264.7 macrophages. Eur. J. Pharmacol. 584, 175–184.

Koyama, S., Sato, E., Masubuchi, T., Takamizawa, A., Kubo, K., Nagai, S., Isumi, T., 1999. Procaterol inhibits IL-1β- and TNF-α-mediated epithelial cell eosinophil chemotactic activity. Eur. Respir. J. 14, 767–775.

Marshansky, V., Vinay, P., 1996. Proton gradient formation in early endosomes from proximal tubes. Biochem. Biophys. Acta 1284, 171–180.

Mellman, I., Fuchs, R., Helenius, A., 1986. Acidification of the endocytic and exocytic pathways. Ann. Rev. Biochem. 55, 663–700.

Nass, R., Rao, R., 1998. Novel localization of a Na^+/H^+ exchanger in a late endosomal compartment of yeast. Implications for vacuole biogenesis. J. Biol. Chem. 273, 21054–21060.

Nolan, T., Hands, R.E., Bustin, S.A., 2006. Quantification of mRNA using real-time RT-PCR. Nat. Protoc. 1, 1559–1582.

Numazaki, Y., Oshima, T., Ohmi, A., Tanaka, A., Oizumi, Y., Komatsu, S., Takagi, T., Karahashi, M., Ishida, N., 1987. A microplate methods for isolation of viruses from infants and children with acute respiratory infections. Microbiol. Immunol. 31, 1085–1095.

O'Donnell, R.A., Richter, A., Ward, J., Angco, G., Mehta, A., Rousseau, K., Swallow, D.M., Holgate, S.T., Djukanovic, R., Davies, D.E., Wilson, S.J., 2004. Expression of ErbB receptors and mucins in the airways of long term current smokers. Thorax 59, 1032–1040.

Oddera, S., Silvestri, M., Lantero, S., Sacco, O., Rossi, G.A., 1998. Downregulation of the expression of intercellular adhesion molecule (ICAM)-1 on bronchial epithelial cells by fenoterol, a β_2-adrenoceptor agonist. J. Asthma 35, 401–408.

Oliveira-Souza, M., Musa-Aziz, R., Malnic, G., De Mello Aires, M., 2004. Arginine vasopressin stimulates H^+-ATPase in MDCK cells via V1 (cell Ca^{2+}) and V2 (cAMP) receptors. Am. J. Physiol. 286, F402–F408.

Papi, A., Johnston, S.L., 1999. Respiratory epithelial cell expression of vascular cell adhesion molecule-1 and its up-regulation by rhinovirus infection via NF-κB and GATA transcription factors. J. Biol. Chem. 274, 30041–30051.

Pérez, L., Carrasco, L., 1993. Entry of poliovirus into cells does not require a low-pH step. J. Virol. 67, 4543–4548.

Pizzichini, M.M.M., Pizzichini, E., Efthimiadis, A., Chauhan, A.J., Johnston, S.L., Hussack, P., Mahony, J., Dolovich, J., Hargreave, F.E., 1998. Asthma and natural colds. Inflammatory indices in induced sputum: a feasibility study. Am. J. Respir. Crit. Care Med. 158, 1178–1184.

Riise, G.C., Larsson, S., Lofdahl, C.G., Andersson, B.A., 1994. Circulating cell adhesion molecules in bronchial lavage and serum in COPD patients with chronic bronchitis. Eur. Respir. J. 7, 1673–1677.

Rogers, D.F., Barnes, P.J., 2006. Treatment of airway mucus hypersecretion. Ann. Med. 38, 116–125.

Sasaki, T., Yamaya, M., Yasuda, H., Inoue, D., Yamada, M., Kubo, H., Nishimura, H., Sasaki, H., 2005. The proton pump inhibitor lansoprazole inhibits rhinovirus infection in cultured human tracheal epithelial cells. Eur. J. Pharmacol. 509, 201–210.

Seemungal, T., Harper-Owen, R., Bhowmik, A., Jeffries, D.J., Wedzicha, J.A., 2000. Detection of rhinovirus in induced sputum at exacerbation of chronic obstructive pulmonary disease. Eur. Respir. J. 16, 677–683.

Silvestri, M., Fregonese, L., Sabatini, F., Dasic, G., Rossi, G.A., 2001. Fluticasone and salmeterol downregulate in vitro, fibroblast proliferation and ICAM-1 or H-CAM expression. Eur. Respir. J. 18, 139–145.

Subauste, M.C., Jacoby, D.B., Richards, S.M., Proud, D., 1995. Infection of a human respiratory epithelial cell line with rhinovirus. Induction of cytokine release and modulation of susceptibility to infection by cytokine exposure. J. Clin. Invest. 96, 549–557.

Suzuki, T., Yamaya, M., Sekizawa, K., Yamada, N., Nakayama, K., Ishizuka, S., Kamanaka, M., Morimoto, T., Numazaki, Y., Sasaki, H., 2000. Effects of dexamethasone on rhinovirus infection in cultured human tracheal epithelial cells. Am. J. Physiol. 278, L560–L571.

Suzuki, T., Yamaya, M., Sekizawa, K., Hosoda, M., Yamada, N., Ishizuka, S., Nakayama, K., Yanai, M., Numazaki, Y., Sasaki, H., 2001. Bafilomycin A_1 inhibits rhinovirus infection in human airway epithelium: effects on endosome and ICAM-1. Am. J. Physiol. 280, L1115–L1127.

Suzuki, T., Yamaya, M., Sekizawa, K., Hosoda, M., Yamada, N., Ishizuka, S., Yoshino, A., Yasuda, H., Takahashi, H., Nishimura, H., Sasaki, H., 2002. Erythromycin inhibits rhinovirus infection in cultured human tracheal epithelial cells. Am. J. Respir. Crit. Care Med. 165, 1113–1118.

Tashimo, H., Yamashita, N., Ishida, H., Nagase, H., Adachi, T., Nakano, J., Yamamura, K., Yano, T., Yoshihara, H., Ohta, K., 2007. Effect of procaterol, a β_2 selective adrenergic receptor agonist, on airway inflammation and hyperresponsiveness. Allergol. Int. 56, 241–247.

Terajima, M., Yamaya, M., Sekizawa, K., Okinaga, S., Suzuki, T., Yamada, N., Nakayama, K., Ohrui, T., Oshima, T., Numazaki, Y., Sasaki, H., 1997. Rhinovirus infection of primary cultures of human tracheal epithelium: role of ICAM-1 and IL-1β. Am. J. Physiol. 273, L749–L759.

Turner, R.B., Couch, R.B., 2006. Rhinoviruses, In: Knipe, D.M., Howley, P.M. (Eds.), Fields Virology, 5th ed. Lippincott Williams and Wilkins, Philadelphia, PA, pp. 895–909.

Yamaya, M., Finkbeiner, W.E., Chun, S.Y., Widdicombe, J.H., 1992. Differentiated structure and function of cultures from human tracheal epithelium. Am. J. Physiol. 262, L713–L724.

Yamaya, M., Sasaki, T., Yasuda, H., Inoue, D., Suzuki, T., Asada, M., Yoshida, M., Seki, T., Iwasaki, K., Nishimura, H., Nakayama, K., 2007. Hochu-ekki-to inhibits rhinovirus infection in human tracheal epithelial cells. Br. J. Pharmacol. 150, 702–710.

Yasuda, H., Yamaya, M., Sasaki, T., Inoue, D., Nakayama, K., Yamada, M., Asada, M., Yoshida, M., Suzuki, T., Nishimura, H., Sasaki, H., 2006. Carbocisteine inhibits rhinovirus infection in human tracheal epithelial cells. Eur. Respir. J. 28, 51–58.

Yoshida, N., Muraguchi, M., Kamata, M., Ikezono, K., Mori, T., 2009. Procaterol potentiates the anti-inflammatory activity of budesonide on eosinophil adhesion to lung fibroblasts. Int. Arch. Allergy Immunol. 150, 352–358.

Zhu, Z., Tang, W., Ray, A., Wu, Y., Einarsson, O., Landry, M.L., Gwaltney Jr., J., Elias, J.A., 1996. Rhinovirus stimulation of interleukin-6 in vivo and in vitro. Evidence for nuclear factor κB-dependent transcriptional activation. J. Clin. Invest. 97, 421–430.

ANTIMICROBIAL AGENTS AND CHEMOTHERAPY, Apr. 2010, p. 1639–1643 Vol. 54, No. 4
0066-4804/10/$12.00 doi:10.1128/AAC.01364-09

Roles of Calcineurin and Crz1 in Antifungal Susceptibility and Virulence of *Candida glabrata*[▽]

Taiga Miyazaki,[1]* Shunsuke Yamauchi,[1] Tatsuo Inamine,[2] Yosuke Nagayoshi,[1] Tomomi Saijo,[1] Koichi Izumikawa,[1] Masafumi Seki,[1] Hiroshi Kakeya,[1] Yoshihiro Yamamoto,[1] Katsunori Yanagihara,[1] Yoshitsugu Miyazaki,[3] and Shigeru Kohno[1]

Department of Molecular Microbiology and Immunology, Nagasaki University School of Medicine, 1-7-1 Sakamoto, Nagasaki 852-8501, Japan[1]; Department of Pharmacotherapeutics, Nagasaki University Graduate School of Biomedical Sciences, 1-14 Bunkyo-machi, Nagasaki 852-8521, Japan[2]; and Department of Bioactive Molecules, National Institutes of Infectious Diseases, 1-23-1 Toyama, Shinjuku-ku, Tokyo 162-8640, Japan[3]

Received 28 September 2009/Returned for modification 15 November 2009/Accepted 15 January 2010

A *Candida glabrata* calcineurin mutant exhibited increased susceptibility to both azole antifungal and cell wall-damaging agents and was also attenuated in virulence. Although a mutant lacking the downstream transcription factor Crz1 displayed a cell wall-associated phenotype intermediate to that of the calcineurin mutant and was modestly attenuated in virulence, it did not show increased azole susceptibility. These results suggest that calcineurin regulates both Crz1-dependent and -independent pathways depending on the type of stress.

Infections caused by the opportunistic fungal pathogen *Candida glabrata* are often difficult to treat due in part to its intrinsic or rapidly acquired resistance to azole antifungals (25). Calcineurin, a serine-threonine-specific protein phosphatase (1), has attracted attention as a new target of antifungal therapy based on studies in several pathogenic fungi, including *Candida albicans*, *Cryptococcus neoformans*, and *Aspergillus fumigatus* (reviewed in reference 31). To date, very little is known about the calcineurin pathway in *C. glabrata*, although it has been reported that azole antifungals and calcineurin inhibitors have mild synergistic effects against *C. glabrata* wild-type strains (8, 15, 22). The transcription factor Crz1 is a downstream effector of calcineurin and is involved in azole tolerance in *C. albicans* (14, 23, 28); however, a Crz1 homolog in *C. glabrata* has yet to be characterized. Therefore, our objective was to evaluate the potential roles of calcineurin and its downstream target Crz1 in antifungal tolerance and virulence of *C. glabrata* through the characterization of mutant phenotypes.

Calcineurin is a heterodimer consisting of a catalytic A subunit and a Ca^{2+}-binding regulatory B subunit, and the association between the two subunits is necessary for phosphatase activity (19). To genetically disrupt calcineurin, we completely deleted the *CNB1* open reading frame (ORF) encoding the regulatory B subunit. *C. glabrata* orthologs of *CNB1* and *CRZ1* were identified in the genome database Génolevures (http://www.genolevures.org/). The primers and strains used in this study are listed in Tables 1 and 2, respectively. *C. glabrata* cells were propagated in minimal medium (0.7% yeast nitrogen base without amino acids, 2% dextrose) at 30°C, unless otherwise noted. Gene deletion was performed by a one-step PCR-based technique as described previously (13). Briefly, a 1-kb XhoI fragment containing *C. glabrata HIS3* was excised from pCgACH (17) and inserted into pBluescript II SK(+) (Stratagene, La Jolla, CA) to yield pBSK-HIS. A deletion construct was amplified from pBSK-HIS with primers tagged with the 100-bp sequences homologous to the flanking regions of the target ORF. Transformation of *C. glabrata* was performed using the lithium acetate protocol (6). Both PCR and Southern blotting were performed to verify that the desired homologous recombination occurred at the target locus without ectopic integration. To construct a centromere-based plasmid containing a *C. glabrata TRP1* marker, a 1,025-bp SacI-KpnI fragment containing the *Saccharomyces cerevisiae PGK1* promoter, a polylinker, and the *C. glabrata HIS3* 3′ flanking region was excised from pGRB2.2 (12) and inserted into the corresponding site of pCgACT (17) to yield pCgACT-P. The entire ORFs of *C. glabrata CNB1* and *CRZ1* were amplified from the genomic DNA of CBS138 (10) and inserted into pCgACT-P to generate pCgACT-PNB and pCgACT-PRZ, respectively. The constructed plasmids were verified by sequencing before use. Complemented strains were made by transforming mutant strains with a plasmid construct containing the corresponding wild-type gene.

To examine the susceptibility of the generated mutants to antifungal agents, MIC assays were performed (Table 3) with a commercially prepared colorimetric microdilution panel (ASTY; Kyokuto Pharmaceutical Industrial Co., Ltd.) (24). Although increased azole susceptibility was observed in the Δ*cnb1* strain, the Δ*crz1* strain displayed susceptibility levels similar to, or in some instances lower than, those of wild-type cells. The *CNB1*-complemented strain displayed recovered azole tolerance. Neither the Δ*cnb1* nor Δ*crz1* strain had an effect on amphotericin B susceptibility. Next, we monitored the percent viability of each strain in the presence and absence of fluconazole as described previously (15). Although the antifun-

* Corresponding author. Mailing address: Department of Molecular Microbiology and Immunology, Nagasaki University School of Medicine, 1-7-1 Sakamoto, Nagasaki 852-8501, Japan. Phone: 81-95-819-7273. Fax: 81-95-849-7285. E-mail: taiga-m@nagasaki-u.ac.jp.

▽ Published ahead of print on 25 January 2010.

TABLE 1. Primers used in this study

Primer[a]	Target gene	Sequence (5′–3′)[b]
For gene deletion		
CgCNB 100-F	*CNB1*	*GTATGTGATGCTTCTCACAGGGTTCAGACGGTTACATACCATCGCTTGAG AGTCATAGTAAATGTTCAGGTTCACGATTAAATCATGCTTTCTCTTTGA* **TAATACGACTCACTATAGGGC**
CgCNB 100-R	*CNB1*	*GCGAACTCTGAAATGTAGATCAAGGATTATTCTGTCCTTGAAATGGGTGT TGATGTCCCTCACTAGGAAAGACAACCACTTTACTATTGTAAGGGGTG A* **CGCTCTAGAACTAGTGGATCC**
CgCRZ 100-F	*CRZ1*	*GATAACGAGTTGGACGCCCTCTTTTGGAAGTCTGTTCTGGTTGCAGATG CTTATAGACCCTGGATCAAGCACTTCATTTCATTGGGATTACAGCTTTT* **CTAATACGACTCACTATAGGGC**
CgCRZ 100-R	*CRZ1*	*CACAATCTTGATTCTGAAGAAAAAAATTTATCATTAAAAATACTGGAGGTT TGTGTTAATTTATTCCAAAGTAACACCCATCTCAGTTGCTTGAATATTCG* **CTCTAGAACTAGTGGATCC**
For gene cloning		
CgCNB1-F2-5P	*CNB1*	ATCAAGGGAAATGGGAGC
CgCNB1-R1-5P	*CNB1*	CGCCCTAAGTTACATCTCTCCTCG
CgCRZ1-F1-E	*CRZ1*	CGGAATTCATGGGCGATAACGAAGAGGA
CgCRZ1-R1938-E	*CRZ1*	CGGAATTCTTATTCCAAAGTAACACCCATCTCA

[a] "F" and "R" indicate forward and reverse primers, respectively.
[b] Sequences homologous to flanking regions of the target ORF are shown in italics. Sequences shown in boldface are present in pBSK-HIS. Restriction sites are underlined.

gal activity of fluconazole is generally fungistatic, the drug was fungicidal for the Δ*cnb1* strain (Fig. 1). In contrast, the deletion of *CRZ1* did not affect the antifungal activity of fluconazole. These results suggest that calcineurin is involved in azole tolerance via a Crz1-independent pathway in *C. glabrata*.

To examine cell wall-associated phenotypes in the Δ*cnb1* and Δ*crz1* strains, we examined their susceptibilities to different types of cell wall-damaging agents, including micafungin (inhibitor of β-1,3-glucan synthesis), Congo red (inhibitor of chitin and β-glucan fiber formation), and calcofluor white (inhibitor of chitin polymer assembly), using a previously described method (15, 20, 26). Micafungin was kindly provided by Astellas (Tokyo, Japan) and dissolved in distilled water. Decreased micafungin tolerance was observed in the Δ*cnb1* and Δ*crz1* strains compared to that in the wild-type control, and this was reversed in the reconstituted strains (Fig. 2). While the Δ*cnb1* strain showed decreased tolerance to both Congo red and calcofluor white, the Δ*crz1* strain exhibited only moderately decreased tolerance to Congo red and was unaffected by calcofluor white exposure (Fig. 2B). These results suggest that the calcineurin-Crz1 pathway plays a role in the response to β-1,3-glucan defects and that calcineurin also regulates a Crz1-independent pathway(s) in response to impaired chitin construction in *C. glabrata*.

To date, the involvement of calcineurin and Crz1 in virulence has not been reported in *C. glabrata*. In contrast to the *C. neoformans* calcineurin mutant (21), deletion of either *CNB1* or *CRZ1* did not affect cell growth at 37°C in *C. glabrata* (data not shown), which is a necessary prerequisite for comparing virulence levels. We therefore performed a virulence assay using a murine model of disseminated candidiasis as described previously (5). Briefly, groups of 10 female, 8-week-old, BALB/c mice (Charles River Laboratories Japan, Inc., Japan) were infected via the lateral tail vein. The mice were euthanized 7 days after injection to determine the number of organ CFU. In this study, no mice died before euthanasia. Statistical analyses were performed using the Kruskal-Wallis test with Dunn's posttest for multiple comparisons. A P value of <0.05 was considered statistically significant. Mice infected with the Δ*cnb1* strain showed significantly reduced fungal burden in all examined organs compared to those infected with the wild-type control and *CNB1*-complemented strains (Fig. 3). Decreased numbers of CFU of the Δ*crz1* strain were statistically significant in the kidney but not in the liver and spleen. The results from this assay indicate that the loss of calcineurin

TABLE 2. Strains used in this study

Strain	Genotype or description	Reference or source
CBS138	Wild type	10
2001T	Δ*trp1* (a derivative of CBS138)	16
2001HT	Δ*his3* Δ*trp1* (made from 2001T)	16
TG11	2001T containing pCgACT-P	This study
TG161	Δ*cnb1*::*HIS3* Δ*trp1* (made from 2001HT)	This study
TG162	TG161 containing pCgACT-P	This study
TG163	TG161 containing pCgACT-PNB	This study
TG171	Δ*crz1*::*HIS3* Δ*trp1* (made from 2001HT)	This study
TG172	TG171 containing pCgACT-P	This study
TG173	TG171 containing pCgACT-PRZ	This study

TABLE 3. Antifungal susceptibilities of *C. glabrata* strains

Strain (genotype)	MIC (μg/ml)[a]				
	FLC	MCZ	ITC	VRC	AMB
TG11 (wild type)	16	0.5	2	0.25	0.5
TG162 (Δ*cnb1*)	4	0.125	0.5	0.125	0.5
TG163 (Δ*cnb1* + *CNB1*)	16	0.5	2	0.25	0.5
TG172 (Δ*crz1*)	32	1	1	0.5	0.5
TG173 (Δ*crz1* + *CRZ1*)	16	0.5	1	0.25	0.5

[a] FLC, fluconazole; MCZ, miconazole; ITC, itraconazole; VRC, voriconazole; AMB, amphotericin B.

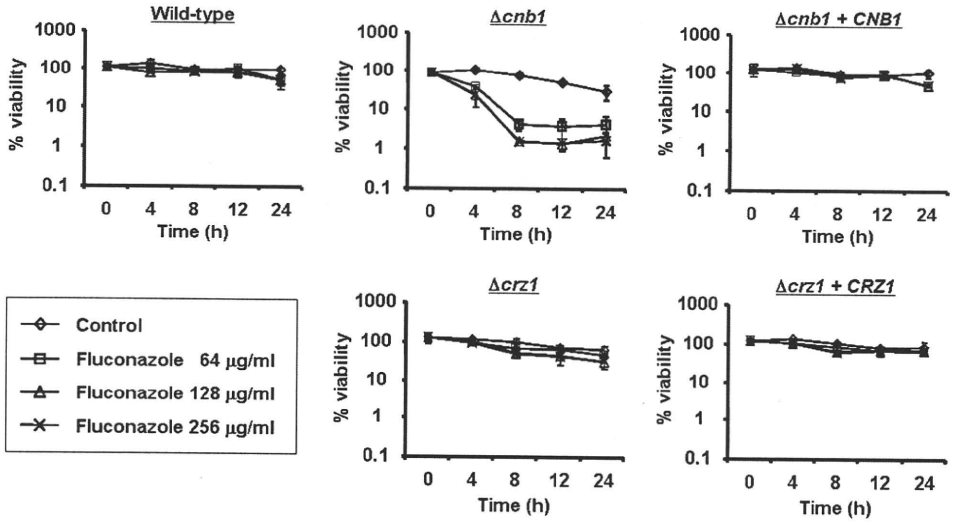

FIG. 1. Time-kill curves of *C. glabrata* wild-type and mutant strains exposed to fluconazole. Logarithmic-phase cells (5×10^5 CFU/ml) were incubated in minimal medium with agitation in the presence or absence of fluconazole at the indicated concentrations. The total number of cells was counted using a hemocytometer, and the number of viable cells was determined by plating the appropriate dilutions on yeast extract-peptone-dextrose (YPD) plates. The data are expressed as the percentages of viability and represent the means and standard deviations for three independent experiments.

results in attenuated virulence while a deletion of *CRZ1* causes only a partial reduction.

This is the first report characterizing the phenotypes of *C. glabrata CNB1* and *CRZ1* mutants, and it has identified both similarities and differences with findings for other fungi. For example, the observed *C. glabrata* Δ*cnb1* strain phenotype, which is characterized by an increased susceptibility to azoles and cell wall-damaging agents as well as decreased virulence, is

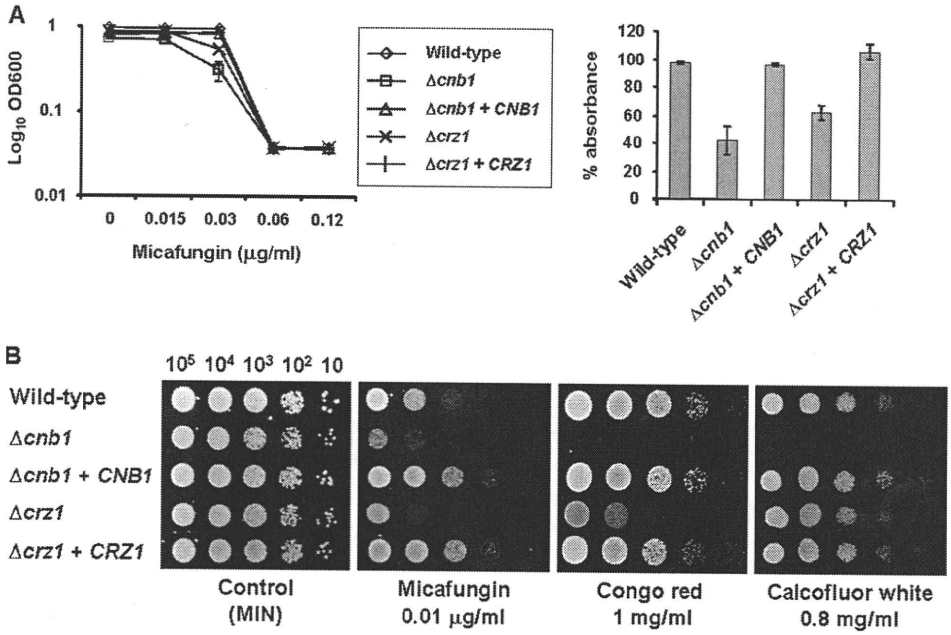

FIG. 2. Susceptibilities of *C. glabrata* wild-type and mutant strains to cell wall-damaging agents. (A) Logarithmic-phase cells (2.5×10^3 CFU/ml) were incubated in minimal medium in either the presence or absence of micafungin, and the optical density at 600 nm (OD_{600}) was measured after 24 h (left panel). The percentages of absorbance were calculated from the OD_{600} of each culture after 24 h of incubation in the presence of 0.03 μg/ml micafungin relative to those in the absence of micafungin (right panel). Data represent the means and standard deviations for three independent experiments. (B) Serial 10-fold dilutions of *C. glabrata* log-phase cells were spotted onto minimal medium (MIN) plates containing micafungin, Congo red, or calcofluor white at the indicated concentrations. Plates were incubated at 30°C for 48 h. All sensitivity tests were repeated at least three times. *C. glabrata* strains were as follows: wild type, strain 2001T containing an empty vector (strain TG11); Δ*cnb1*, a Δ*cnb1* strain containing an empty vector (strain TG162); Δ*cnb1* + *CNB1*, a *CNB1*-complemented strain made with pCgACT-PNB (strain TG163); Δ*crz1*, a Δ*crz1* strain containing an empty vector (strain TG172); and Δ*crz1* + *CRZ1*, a *CRZ1*-complemented strain made with pCgACT-PRZ (strain TG173).

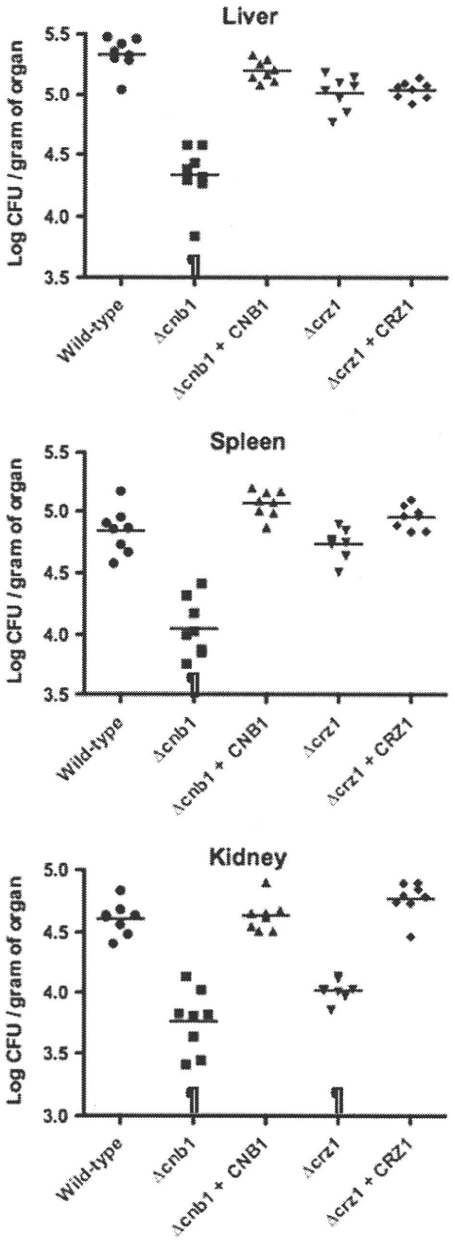

FIG. 3. Virulence assay using a mouse model of disseminated candidiasis. Groups of 10 mice were intravenously inoculated with 8×10^7 cells for each *C. glabrata* strain. Three target organs (liver, spleen, and bilateral kidneys) were excised 7 days after injection. Appropriate dilutions of organ homogenates were plated, and the numbers of CFU were counted after 3 days of incubation at 30°C. Numbers of recovered CFU from each organ are indicated for individual mice in the scatter plots. The geometric mean is shown as a bar. Representative data of two independent experiments are shown. *C. glabrata* strains are as follows: wild type, strain TG11 (wild-type control) (filled circles); Δ*cnb1*, TG162 (Δ*cnb1* strain containing an empty vector) (squares); Δ*cnb1* + *CNB1*, TG163 (*CNB1*-complemented strain made with pCgACT-PNB) (triangles); Δ*crz1*, TG172 (Δ*crz1* strain containing an empty vector) (inverted triangles); Δ*crz1* + *CRZ1*, TG173 (*CRZ1*-complemented strain made with pCgACT-PRZ) (diamonds). ¶, $P < 0.05$ (Kruskal-Wallis test with Dunn's posttest).

consistent with previous findings for other pathogenic fungi, such as *C. albicans* (2–4, 27), *C. neoformans* (11, 18, 21), and *A. fumigatus* (9, 30). To date, an ortholog of Crz1 in *C. neoformans* has not been identified and a mutant phenotype associated with azole susceptibility in *A. fumigatus* has yet to be reported; thus, the full importance of this transcriptional factor is not clear for these fungi. Although the virulence of a Δ*crz1* mutant is highly attenuated in *A. fumigatus* (7, 29), this mutation has little effect on virulence in both *C. albicans* (14, 23) and *C. glabrata* (Fig. 3). In contrast to that in *C. albicans* (14, 23, 28), the loss of Crz1 did not result in increased azole susceptibility in *C. glabrata*. In addition, the *C. glabrata* Δ*crz1* strain exhibited increased susceptibility to micafungin and Congo red but not to calcofluor white. Taken together, these results indicate that calcineurin-mediated Crz1 regulation is dependent upon the type of stress and that the regulatory mechanisms vary among fungal species. Further characterization of these mutant phenotypes will help to discover a novel and conserved calcineurin target in pathogenic fungi.

We thank Hironobu Nakayama for providing *C. glabrata* strains 2001T and 2001HT and plasmids pCgACH and pCgACT and Brendan Cormack for providing pGRB2.2.

This research was partially supported by a Grant-in-Aid for Scientific Research (no. 19790324 to T.M. and no. 21390305 to S.K.) from the Japanese Ministry of Education, Culture, Sports, Science and Technology, a grant from the Global Centers of Excellence Programs, Nagasaki University, and grants from the Ministry of Health, Labor and Welfare (H20-nanchi-ippan-035, H20-shinko-ippan-012, and H20-shinko-ippan-015 to Y.M.).

REFERENCES

1. **Aramburu, J., A. Rao, and C. B. Klee.** 2000. Calcineurin: from structure to function. Curr. Top. Cell. Regul. **36:**237–295.
2. **Bader, T., B. Bodendorfer, K. Schroppel, and J. Morschhauser.** 2003. Calcineurin is essential for virulence in Candida albicans. Infect. Immun. **71:** 5344–5354.
3. **Bader, T., K. Schroppel, S. Bentink, N. Agabian, G. Kohler, and J. Morschhauser.** 2006. Role of calcineurin in stress resistance, morphogenesis, and virulence of a Candida albicans wild-type strain. Infect. Immun. **74:**4366–4369.
4. **Blankenship, J. R., F. L. Wormley, M. K. Boyce, W. A. Schell, S. G. Filler, J. R. Perfect, and J. Heitman.** 2003. Calcineurin is essential for Candida albicans survival in serum and virulence. Eukaryot. Cell **2:**422–430.
5. **Chen, K. H., T. Miyazaki, H. F. Tsai, and J. E. Bennett.** 2007. The bZip transcription factor Cgap1p is involved in multidrug resistance and required for activation of multidrug transporter gene CgFLR1 in Candida glabrata. Gene **386:**63–72.
6. **Cormack, B. P., and S. Falkow.** 1999. Efficient homologous and illegitimate recombination in the opportunistic yeast pathogen Candida glabrata. Genetics **151:**979–987.
7. **Cramer, R. A., Jr., B. Z. Perfect, N. Pinchai, S. Park, D. S. Perlin, Y. G. Asfaw, J. Heitman, J. R. Perfect, and W. J. Steinbach.** 2008. Calcineurin target CrzA regulates conidial germination, hyphal growth, and pathogenesis of Aspergillus fumigatus. Eukaryot. Cell **7:**1085–1097.
8. **Cruz, M. C., A. L. Goldstein, J. R. Blankenship, M. Del Poeta, D. Davis, M. E. Cardenas, J. R. Perfect, J. H. McCusker, and J. Heitman.** 2002. Calcineurin is essential for survival during membrane stress in Candida albicans. EMBO J. **21:**546–559.
9. **da Silva Ferreira, M. E., T. Heinekamp, A. Hartl, A. A. Brakhage, C. P. Semighini, S. D. Harris, M. Savoldi, P. F. de Gouvea, M. H. de Souza Goldman, and G. H. Goldman.** 2007. Functional characterization of the Aspergillus fumigatus calcineurin. Fungal Genet. Biol. **44:**219–230.
10. **Dujon, B., D. Sherman, G. Fischer, P. Durrens, S. Casaregola, I. Lafontaine, J. De Montigny, C. Marck, C. Neuveglise, E. Talla, N. Goffard, L. Frangeul, M. Aigle, V. Anthouard, A. Babour, V. Barbe, S. Barnay, S. Blanchin, J. M. Beckerich, E. Beyne, C. Bleykasten, A. Boisrame, J. Boyer, L. Cattolico, F. Confanioleri, A. De Daruvar, L. Despons, E. Fabre, C. Fairhead, H. Ferry-Dumazet, A. Groppi, F. Hantraye, C. Hennequin, N. Jauniaux, P. Joyet, R. Kachouri, A. Kerrest, R. Koszul, M. Lemaire, I. Lesur, L. Ma, H. Muller, J. M. Nicaud, M. Nikolski, S. Oztas, O. Ozier-Kalogeropoulos, S. Pellenz, S. Potier, G. F. Richard, M. L. Straub, A. Suleau, D. Swennen, F. Tekaia, M. Wesolowski-Louvel, E. Westhof, B. Wirth, M. Zeniou-Meyer, I. Zivanovic,**

M. Bolotin-Fukuhara, A. Thierry, C. Bouchier, B. Caudron, C. Scarpelli, C. Gaillardin, J. Weissenbach, P. Wincker, and J. L. Souciet. 2004. Genome evolution in yeasts. Nature **430**:35–44.

11. **Fox, D. S., M. C. Cruz, R. A. Sia, H. Ke, G. M. Cox, M. E. Cardenas, and J. Heitman.** 2001. Calcineurin regulatory subunit is essential for virulence and mediates interactions with FKBP12-FK506 in Cryptococcus neoformans. Mol. Microbiol. **39**:835–849.
12. **Frieman, M. B., J. M. McCaffery, and B. P. Cormack.** 2002. Modular domain structure in the Candida glabrata adhesin Epa1p, a beta1,6 glucan-cross-linked cell wall protein. Mol. Microbiol. **46**:479–492.
13. **Gola, S., R. Martin, A. Walther, A. Dunkler, and J. Wendland.** 2003. New modules for PCR-based gene targeting in Candida albicans: rapid and efficient gene targeting using 100 bp of flanking homology region. Yeast **20**: 1339–1347.
14. **Karababa, M., E. Valentino, G. Pardini, A. T. Coste, J. Bille, and D. Sanglard.** 2006. CRZ1, a target of the calcineurin pathway in Candida albicans. Mol. Microbiol. **59**:1429–1451.
15. **Kaur, R., I. Castano, and B. P. Cormack.** 2004. Functional genomic analysis of fluconazole susceptibility in the pathogenic yeast Candida glabrata: roles of calcium signaling and mitochondria. Antimicrob. Agents Chemother. **48**: 1600–1613.
16. **Kitada, K., E. Yamaguchi, and M. Arisawa.** 1995. Cloning of the Candida glabrata TRP1 and HIS3 genes, and construction of their disruptant strains by sequential integrative transformation. Gene **165**:203–206.
17. **Kitada, K., E. Yamaguchi, and M. Arisawa.** 1996. Isolation of a Candida glabrata centromere and its use in construction of plasmid vectors. Gene **175**:105–108.
18. **Kraus, P. R., D. S. Fox, G. M. Cox, and J. Heitman.** 2003. The Cryptococcus neoformans MAP kinase Mpk1 regulates cell integrity in response to antifungal drugs and loss of calcineurin function. Mol. Microbiol. **48**:1377–1387.
19. **Kraus, P. R., and J. Heitman.** 2003. Coping with stress: calmodulin and calcineurin in model and pathogenic fungi. Biochem. Biophys. Res. Commun. **311**:1151–1157.
20. **Miyazaki, T., H. F. Tsai, and J. E. Bennett.** 2006. Kre29p is a novel nuclear protein involved in DNA repair and mitotic fidelity in Candida glabrata. Curr. Genet. **50**:11–22.
21. **Odom, A., S. Muir, E. Lim, D. L. Toffaletti, J. Perfect, and J. Heitman.** 1997. Calcineurin is required for virulence of Cryptococcus neoformans. EMBO J. **16**:2576–2589.
22. **Onyewu, C., J. R. Blankenship, M. Del Poeta, and J. Heitman.** 2003. Ergosterol biosynthesis inhibitors become fungicidal when combined with calcineurin inhibitors against Candida albicans, Candida glabrata, and Candida krusei. Antimicrob. Agents Chemother. **47**:956–964.
23. **Onyewu, C., F. L. Wormley, Jr., J. R. Perfect, and J. Heitman.** 2004. The calcineurin target, Crz1, functions in azole tolerance but is not required for virulence of Candida albicans. Infect. Immun. **72**:7330–7333.
24. **Pfaller, M. A., S. Arikan, M. Lozano-Chiu, Y. Chen, S. Coffman, S. A. Messer, R. Rennie, C. Sand, T. Heffner, J. H. Rex, J. Wang, and N. Yamane.** 1998. Clinical evaluation of the ASTY colorimetric microdilution panel for antifungal susceptibility testing. J. Clin. Microbiol. **36**:2609–2612.
25. **Pfaller, M. A., and D. J. Diekema.** 2007. Epidemiology of invasive candidiasis: a persistent public health problem. Clin. Microbiol. Rev. **20**:133–163.
26. **Ram, A. F., and F. M. Klis.** 2006. Identification of fungal cell wall mutants using susceptibility assays based on Calcofluor white and Congo red. Nat. Protoc. **1**:2253–2256.
27. **Sanglard, D., F. Ischer, O. Marchetti, J. Entenza, and J. Bille.** 2003. Calcineurin A of Candida albicans: involvement in antifungal tolerance, cell morphogenesis and virulence. Mol. Microbiol. **48**:959–976.
28. **Santos, M., and I. F. de Larrinoa.** 2005. Functional characterization of the Candida albicans CRZ1 gene encoding a calcineurin-regulated transcription factor. Curr. Genet. **48**:88–100.
29. **Soriani, F. M., I. Malavazi, M. E. da Silva Ferreira, M. Savoldi, M. R. Von Zeska Kress, M. H. de Souza Goldman, O. Loss, E. Bignell, and G. H. Goldman.** 2008. Functional characterization of the Aspergillus fumigatus CRZ1 homologue, CrzA. Mol. Microbiol. **67**:1274–1291.
30. **Steinbach, W. J., R. A. Cramer, Jr., B. Z. Perfect, Y. G. Asfaw, T. C. Sauer, L. K. Najvar, W. R. Kirkpatrick, T. F. Patterson, D. K. Benjamin, Jr., J. Heitman, and J. R. Perfect.** 2006. Calcineurin controls growth, morphology, and pathogenicity in Aspergillus fumigatus. Eukaryot. Cell **5**:1091–1103.
31. **Steinbach, W. J., J. L. Reedy, R. A. Cramer, Jr., J. R. Perfect, and J. Heitman.** 2007. Harnessing calcineurin as a novel anti-infective agent against invasive fungal infections. Nat. Rev. Microbiol. **5**:418–430.

Medical Mycology June 2010, **48**, 606–612

informa
healthcare

Anti-*Candida*-biofilm activity of micafungin is attenuated by voriconazole but restored by pharmacological inhibition of Hsp90-related stress responses

YUKIHIRO KANEKO*, HIDEAKI OHNO*, HIDESUKE FUKAZAWA*, YUKO MURAKAMI*, YOSHIFUMI IMAMURA†, SHIGERU KOHNO† & YOSHITSUGU MIYAZAKI*

**Department of Chemotherapy and Mycosis, National Institute of Infectious Diseases, Tokyo, Japan, and †Department of Molecular Microbiology & Immunology, Nagasaki University Graduate School of Biomedical Sciences, Nagasaki, Japan.*

We have conducted an *in vitro* evaluation of the efficacy of a voriconazole-micafungin combination against *Candida albicans*. When used alone, both micafungin and voriconazole decreased the metabolic activity of planktonic cells, but only micafungin displayed potent anti-biofilm activity. Their combination appeared to have an additive effect against planktonic cells. However, voriconazole significantly antagonized the fungicidal effect of micafungin against *Candida* biofilms. Time-lag experiments showed that pretreatment with voriconazole induced resistance to micafungin in *Candida* biofilms. The micafungin-antagonizing effect of voriconazole persisted even when the biofilm was no longer exposed to voriconazole. In contrast, voriconazole addition after 24 h of micafungin treatment did not alter micafungin sensitivity. To investigate the mechanism of antagonism, we used inhibitors of Hsp90 and its effectors because Hsp90 seems to be implicated in the resistance to micafungin. These molecules reversed the voriconazole-induced resistance to micafungin which suggests that Hsp90-related stress responses are involved in the antagonism. Our results may provide clues as to the mechanism of increased drug resistance in *Candida* biofilms and raises concerns about the use of the voriconazole-micafungin combination in clinical settings.

Keywords *Candida*, biofilm, Hsp90, voriconazole, micafungin

Introduction

The use of long-term implants in clinical practice has been shown to promote colonization and biofilm formation [1]. *Candida albicans* (*C. albicans*) is a pathogen associated with biofilm-related diseases, as well as the primary cause of systemic candidiasis. It is known that the latter has a high mortality rate [2]. Unfortunately, only a limited number of antifungal drugs are available for use in *Candida* infections and the formation of biofilms renders these infections intractable [3]. The common treatment approach in cases of biofilm formation is to remove the implants as soon as possible, but removal is not always possible as is the case with pacemakers or artificial heart valves [4]. Besides, biofilm-related infections may remain unnoticed when they are refractory to intensive antifungal therapy because alternative treatments need to be considered and it is not always possible to confirm the presence of biofilms. Therefore, it is necessary to develop highly effective antifungal drugs against such infections, as well as to utilize existing antifungal agents more effectively.

Combination therapy is a good option in this regard because it is thought to be appropriate for intractable infections [5]. Several new commercially available safe antifungal agents can be considered for combination therapy [6]. As expected, combinations of new azoles and echinocandins have been reported to exert an additive or synergistic effect against most *Candida* species [7]. However, this effect is limited to growth inhibition, and some *in vitro* studies have shown that azoles antagonized the fungicidal effect of echinocandins, especially in biofilms [8–10]. The mechanism underlying this antagonistic effect has never been

Received 17 July 2009; Received in final revised form 9 September 2009; Accepted 19 October 2009

Correspondence: Y. Kaneko, Department of Chemotherapy and Mycosis, National Institute of Infectious Diseases, Toyama 1-23-1, Shinjuku-ku, Tokyo 162-8640, Japan. Tel: +81 (0)3 5285-1111 (2327), fax: +81 (0)3 5285-1272; E-mail: ykaneko@nih.go.jp

DOI: 10.3109/13693780903426721

reported. Our previous study showed that resistance to high doses of micafungin (MFG) (known as the paradoxical effect) is related to heat shock protein 90 (Hsp90) stress responses [11]. This therefore led us to explore the relationship between Hsp90-related stress responses and the antagonistic effect of voriconazole (VRC) against MFG.

Materials and methods

Strains and growth conditions

All strains used in this study were from our laboratory collection. A standard *C. albicans* strain, namely, SC5314, was employed in most experiments. *C. albicans* strains ATCC 10261 and ATCC 10231 and *C. glabrata* strain CG1 were also used in some experiments. All strains were grown in yeast nitrogen base with 2% dextrose (YNB) broth.

Biofilm formation

Biofilms were prepared using a slightly modified version of a previously described method [12]. Briefly, small silicone elastomer (SE) disks (diameter, 4 mm; thickness, 1 mm) were immersed in a *Candida* cell suspension for 90 min to allow attachment, and biofilms were allowed to form by further incubating the disks in YNB for 24 h. We used SE disks that were smaller than those used in previous experiments so that they could be placed in 96-well microplates.

Antifungal agents, inhibitors, and treatment

MFG and VRC were kindly provided by Astellas Pharma Inc. (Japan) and Pfizer Japan Inc. (Japan), respectively. Radicicol (Rad; an Hsp90 inhibitor), cyclosporin A (CsA; a calcineurin inhibitor), and nikkomycin Z (NZ; a chitin synthase inhibitor) were purchased from Sigma-Aldrich (USA), and cercosporamide (Cer; a PKC1 inhibitor) was purchased from BioAustralis Fine Chemicals (Australia). MFG and NZ were dissolved in distilled water, whereas VRC, Rad, CsA, and Cer were dissolved in dimethylsulfoxide (DMSO). These were stored at –30 °C as stock solutions until use at concentrations of 10 mg/ml (MFG, VRC, and NZ), 1 mM (Rad and Cer), and 10 mM (CsA). The final concentrations have been indicated in the sections describing individual experiments. The biofilms on the SE disks were soaked in the medium containing drugs and incubated at 37 °C for 24 h. The minimum inhibitory concentrations (MICs) of MFG, VRC, Rad, CsA, Cer, and NZ against the planktonic cells were determined in flat bottom, 96-well microtiter plates using a broth microdilution protocol modified from the CLSI M27-A standard [13]. Studies to assess MICs were prepared in YNB medium (a total volume of 0.2ml/well) containing each drug. Cell densities of overnight cultures were determined and dilutions were prepared such that approximately 2×10^3 cells were inoculated into each well. MICs of MFG, VRC, Rad, CsA, Cer, and NZ against the planktonic cells were 0.031 μg/ml, 0.008 μg/ml, 8 μM, >80 μM, >8 μM, and 6.25 μg/ml, respectively.

Quantification of biofilms

The metabolic activities of cells in the biofilms were quantified by performing a 3-bis(2-methoxy-4-nitro-5-sulfo-phenyl)-2H-tetrazolium-5-carboxanilide (XTT) reduction assay as previously described [14]. Briefly, after treatment, the medium was removed carefully, and 200 μl of 50 μg/ml XTT and 4 μM menadione in phosphate-buffered saline (PBS) was added to biofilms on the SE disks in each well. The plates were incubated for 1 h at 37 °C, and the absorption of each well at 490 nm (reference 630 nm) was read by using a plate reader. The results were normalized to control (untreated), and the relative metabolic activity of cells was expressed as the percent of the activity in control cells (% control).

To quantify the biomass of biofilms, dry weight measurements and crystal violet (CV) assays were performed. For dry weights, biofilms on SE disks were scraped and transferred onto the preweighed filter papers, and the filter papers with biofilms were dried and weighed. For CV assays, biofilms were briefly dried and then stained with 200 μl of 0.05% CV for 15 min. The disks were rinsed by repeated submersion in distilled water until CV was no longer observed in the rinse water. The disks were dried at 25 °C, and the remaining CV was solubilized with 200 μl of 30% ethanol with 1mM hydrochloride for 10 min at 25 °C. The remaining CV was quantified by measuring absorbance at 570 nm in a plate reader.

Relative Quantification by Real-Time Reverse Transcription-Polymerase Chain Reaction (RT-PCR)

The total RNAs were respectively isolated using the hot phenol method as described elsewhere [15]. To synthesize cDNA, approximately 800 ng of total RNA was used as the template with normalization to actin (*ACT1*) mRNA levels. Gene expression levels of *UTR2* were measured using Applied Biosystems 7000 Real Time PCR System (TaqMan). RT-PCR was performed in 96-well optical reaction plates in quadruplicate (each reaction containing 1xSYBR Green PCR Master mix (invitrogen, USA), 0.15 pmol/ml forward primer and reverse primer and 1 µl template cDNA in a final volume of 10 µl). *ACT1* served as the internal control. Cycling profile included 40 cycles of 95 °C for 5 s, 55 °C for 30 s and 72 °C for 30 s. Data acquisition and the analysis of the real-time PCR assay were performed using the 7000 System SDS Software Version 1.0 (Applied Biosystems). Primers ACT1-for (5′- TTGGTGATGAAGCCCAATCC -3′) and ACT1-rev

(5′-CATATCGTCCCAGTTGGAAAC-3′) were used for amplification of *ACT1*, and primers UTR2-for (5′-GATTCT GGTAGTAGTGGAAGCAGTTCT-3′) and UTR2-rev (5′-ATGGAAGCAAATATACCACTGATAACAC-3′) were used for amplification of *UTR2*.

Statistical Analysis

The data were analyzed by using Mann-Whitney *U* tests. Unless otherwise indicated, the data are presented as the mean ± standard deviation (SD) of 4 or more replicates. The error bars represent the SD. The data are representative of 2 or more individual experiments.

Results

VRC attenuated the effect of MFG against Candida biofilms

We examined whether VRC attenuated the effect of MFG against biofilms in our model. VRC alone decreased XTT activity of biofilms, but the decrease was never below 50% (Fig. 1a). MFG alone greatly reduced biofilm XTT activity

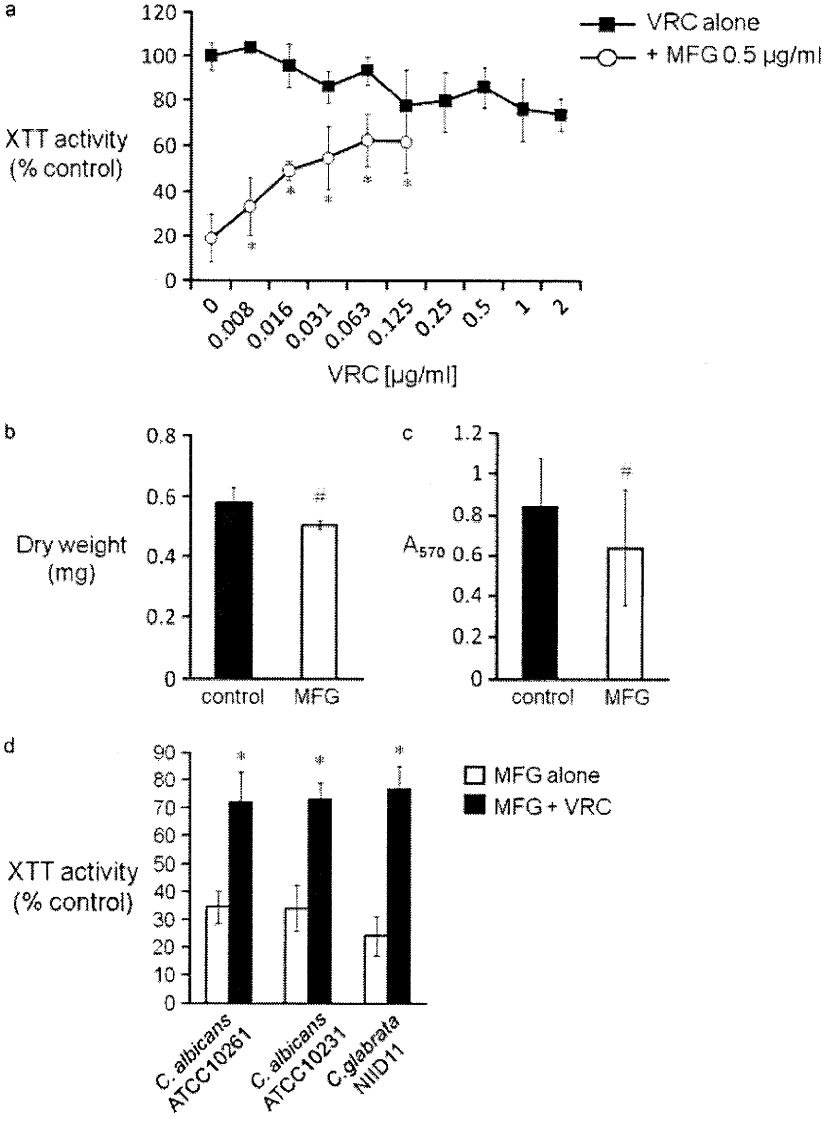

Fig. 1 VRC attenuates the effect of MFG against *Candida* biofilms. (a) 0.5 μg/ml of MFG alone reduces the relative metabolic activity of cells in biofilms by approximately 80% to 90%. The effect of MFG is attenuated by VRC, and the metabolic activity gradually increased up to 60% to 70% dose-dependently. VRC alone decreased the metabolic activity of the cells in the biofilms, but the decrease was never below 50%. Data are representative of 3 independent experiments. (b)(c) MFG alone reduces biomasses when compared with measurements of dry weights (b) and CV assay (c). (d) VRC also attenuates the effect of MFG against the biofilms of 3 strains other than SC5314 that form biofilms as well. VRC, voriconazole; MFG, micafungin; Rad, radicicol; CsA, cyclosporine A; Cer, cercosporamide; NZ, nikkomycin Z; CV, crystal violet. $*P < 0.05$ compared to MFG alone. $\#P < 0.05$ compared to control.

by 80% to 90% at a concentration of 0.5 μg/ml (Fig. 1a). However, addition of VRC attenuated the effect of MFG against biofilms and gradually increased the XTT activity dose-dependently up to 60% to 70% (Fig. 1a). In contrast, this combination showed additive effects against planktonic cells (data not shown) which is consistent with previous reports [7]. Thus, VRC, in cooperation with MFG, inhibits the growth of planktonic cells, but attenuates the effect of MFG against cells in biofilms. We also assessed the effects of MFG by measuring biomass. In both weight measurements and CV assays, MFG reduced biomass, but the effect was less than what was observed in XTT assay (Fig. 1b, c). These results imply that biomass could include living as well as dead cells, along with extracellular matrices. In order to examine whether this antagonistic effect was restricted to only SC5314 strain, we studied several other strains. While some of them did not form biofilms well, VRC attenuated the effect of MFG against biofilms of all 3 strains noted in the methods section (Fig. 1d).

A very high concentration of MFG was required to reverse the antagonistic effect of VRC

To determine the concentration of MFG that could reverse the antagonistic effect of VRC, we increased the doses of MFG added to biofilms in the presence of VRC (0.125 μg/ml). Surprisingly, even a high concentration of 64 μg/ml of MFG in the presence of VRC was not sufficient to exceed the effect of 0.5 μg/ml of MFG alone (Fig. 2). This shows that biofilms become highly resistant to MFG in the presence of VRC, and even an increased dose of MFG could not disrupt biofilms effectively.

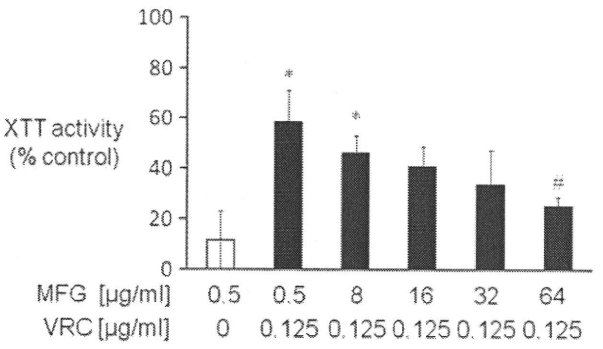

Fig. 2 A very high concentration of MFG is required to reverse the VRC-induced antagonism of MFG against biofilms. MFG reduces the metabolic activity dose-dependently in the presence of VRC, but very high doses of MFG are required to restore the effect of a low dose of MFG alone. VRC, voriconazole; MFG, micafungin. $*P < 0.05$ compared to 0.5 μg/ml of MFG alone. $\#P < 0.05$ compared to 0.5 μg/ml of MFG + 0.125 μg/ml of VRC.

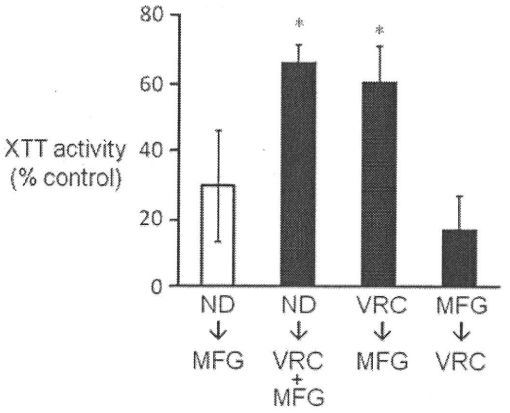

Fig. 3 Combination therapy with a time lag shows that VRC attenuates the effect of MFG even when the biofilm is no longer exposed to VRC. Each bar shows the mean percent of XTT activity compared to control (% control, $n = 8$ each). VRC alone (ND → VRC), the simultaneous combination of VRC and MFG (ND → VRC+MFG), and the serial combination of VRC followed by MFG (VRC → MFG) were less effective than MFG alone (ND → MFG) and the serial combination of MFG followed by VRC (MFG → VRC). There was no significant difference between ND → MFG and MFG → VRC. Data are representative of 3 independent experiments. ND, no drug; VRC, voriconazole; MFG, micafungin; ND → MFG, ND followed by MFG; ND → VRC + MFG, ND followed by VRC + MFG; VRC → MFG, VRC followed by MFG; MFG → VRC, MFG followed by VRC. $*P < 0.05$ compared to 0.5 μg/ml of MFG alone (ND → MFG).

The effect of a serial combination of VRC and MFG was also inferior to that of MFG alone

We added in our studies VRC and MFG sequentially with a time lag in between to examine whether the effect of MFG against biofilms is attenuated even when the biofilm is no longer exposed to VRC. The biofilms were first treated with VRC alone, MFG alone, or no drug (ND) for the first 24 h, and then sequentially with MFG alone, VRC alone, or a combination of VRC and MFG, respectively, for the next 24 h. The concentrations of MFG and VRC were 0.5 μg/ml and 0.125 μg/ml, respectively. The effects of a simultaneous combination of MFG and VRC (ND → VRC+MFG) and the serial combination of VRC followed by MFG (VRC → MFG) were less than that observed with MFG alone. This result shows that the effect of MFG is attenuated even when the biofilm is no longer exposed to VRC (Fig. 3). In contrast, the sequential treatment with MFG followed by VRC (MFG → VRC) was still as effective as MFG alone.

Inhibiting stress responses enhanced the effect of MFG against biofilms and reversed the antagonistic effect of VRC

The results of the time-lag experiment indicated that certain stress responses to VRC possibly modulated the sensitivity of biofilms to MFG. To investigate whether